From the Rolf Luft Research Center for Diabetes and Endocrinology
Department of Molecular Medicine and Surgery
Karolinska Institutet, Stockholm, Sweden

IN VIVO IMAGING OF ISLET CELLS AND ISLET REVASCULARIZATION

Daniel Nyqvist

Karolinska Institutet

Stockholm 2007

Cover image: 3D reconstruction of an image stack captured by *in vivo* TPLSM of one islet engrafted in the anterior chamber of the eye four month after transplantation. Green represents GFP expressing β-cells and red represents Texas Red in the blood vessels. Scale in μm.

Published by Karolinska Institutet.

Published and printed by
REPROPRINT AB
Stockholm 2007
www.reproprint.se
Gårdsvägen 4, 169 70 Solna

ISBN 978-91-7357-116-6

To my family

ABSTRACT

Glucose homeostasis depends on the release of insulin from the pancreatic β-cell. Impaired insulin release is a hallmark of diabetes mellitus. The β-cells are situated within the endocrine pancreas, the islets of Langerhans, which are structurally defined microorgans that create a unique microenvironment required for adequate β-cell function. Pancreatic islet transplantation has emerged as a treatment of type 1 diabetes, but is currently hampered by poor long-term function of transplanted islets. Today, alternatives to monitor islet cell function after transplantation are lacking. Therefore, the aim of this thesis was to develop experimental models that facilitate functional studies of islet cells and islet revascularization after pancreatic islet transplantation under *in vivo* conditions using fluorescence imaging techniques. Laser-scanning microscopy (LSM) enabled fluorescence imaging in intact islet grafts and functional studies of β-cells and the islet graft vasculature. LSM was combined with two different transplantation models; *ex vivo* imaging of islets transplanted under the kidney capsule, and non-invasive *in vivo* imaging of islets transplanted to the anterior chamber of the eye.

To facilitate identification and studies of donor islets after transplantation, the fluorescent reporter expression and function of pancreatic islets were characterized in transgenic YC-3.0 mice. Pancreatic islets in YC-3.0 mice expressed the enhanced yellow fluorescent protein (EYFP), displayed normal β-cell mass and glucose stimulated insulin release *in vitro* and *in vivo*. Furthermore, YC-3.0 islets reversed diabetes and were identified by EYFP fluorescence after transplantation.

Islet isolation disrupts vascular connections and thus delivery of oxygen and nutrients to islet cells. Revascularization is therefore vital for the survival and function of transplanted islets. Transgenic Tie2-green fluorescence protein (GFP) mice, characterized by endothelial cell (EC) specific expression of GFP, were used as islet donors. Living ECs were studied in intact Tie2-GFP islets after isolation and during culture. Intraislet ECs survived islet isolation, but rapidly disappeared during islet culture. After transplantation, LSM imaging revealed that donor islet ECs (DIECs) integrated with recipient ECs and formed functional blood vessels during the revascularization of Tie2-GFP islets. Since islet grafts have a deficient vasculature, we investigated if contributing DIECs improved the revascularization of transplanted islets. Freshly isolated and cultured Tie2-GFP islets were therefore transplanted and the contribution of DIECs to the vasculature was determined, as well as the degree of total vascularization and the revascularization rate of the islet grafts. DIECs contributed to the vasculature of fresh but not cultured islet grafts, and fresh islet grafts revascularized faster compared to cultured islet grafts, indicating reduced exposure to hypoxia for fresh islets. However, after completed revascularization the total vascular density was similar in the two groups.

Pancreatic islets with β-cell specific expression of GFP were transplanted to the anterior chamber of the eye. LSM facilitated non-invasive imaging of GFP fluorescent β-cells in the engrafted islets. Repetitive imaging facilitated longitudinal studies of islet engraftment and revascularization. Furthermore, β-cell death could be non-invasively monitored in transplanted islets during normal and diabetic conditions.

The results in this thesis establish the basis for non-invasive *in vivo* functional investigations of islet cell physiology and islet revascularization after pancreatic islet transplantation, which can be performed longitudinally under normal and diabetic conditions.

LIST OF PUBLICATIONS

This thesis is based on the following papers, which in the text will be referred to by their Roman numerals:

I. Nyqvist D, Mattsson G, Köhler M, Lev-Ram V, Andersson A, Carlsson PO, Nordin A, Berggren PO and Jansson L. Pancreatic islet function in a transgenic mouse expressing fluorescent protein. *Journal of Endocrinology*, 2005, 186, 333-41

II. Nyqvist D, Köhler M, Wahlstedt H and Berggren PO. Donor islet endothelial cells participate in formation of functional vessels within pancreatic islet grafts. *Diabetes*, 2005, 54, 2287-93

III. Nyqvist D and Berggren PO. Donor islet endothelial cells in pancreatic islet revascularization. *Manuscript*.

IV. Nyqvist D, Speier S, Moede T, Köhler M, Leibiger IB, Caicedo A and Berggren PO. *In vivo* imaging of β-cell function and islet revascularization. *Manuscript*.

Related publications and manuscripts:

Lau J, Mattsson M, Nyqvist D, Köhler M, Berggren PO, Jansson L and Carlsson PO. Induced dysfunction in intraportally transplanted pancreatic islets by the liver microenvironment. *Submitted manuscript.*

Seth E, Nyqvist D, Andersson A, Carlsson PO, Köhler M, Mattsson G, Nordin A, Berggren PO and Jansson L. Distribution of intraportally implanted microspheres and fluorescent islets in the liver of mice. *Cell Transplantation, in press*.

Köhler M, Nyqvist D, Moede T, Wahlstedt H, Cabrera C, Leibiger I and Berggren PO. Imaging of Pancreatic Beta-Cell Signal-Transduction. *Curr.Med.Chem.-Immun., Endoc.& Metab. Agents*, 2004, 4, 281-299.

CONTENTS

LIST OF ABBREVIATIONS

AOBS	acousto optical beam splitter
APC	allophycocyanin
$[Ca^{2+}]_i$	cytoplasmic free Ca^{2+} concentration
confocal microscopy	confocal laser-scanning microscopy
DAPI	4',6-diamidino-2-phenylindole
DIEC	donor islet endothelial cell
EC	endothelial cell
ECGS	endothelial cell growth supplement
EYFP	enhanced yellow fluorescence protein
FITC	fluorescein isothiocyanate
4D	four dimensional
FRET	fluorescence resonance energy transfer
FCS	fetal calf serum
FGF	fibroblast growth factor
GFP	green fluorescence protein
GLUT	glucose transporter
LSM	laser-scanning microscopy
VEGF	vascular endothelial growth factor
PBS	phosphate buffered saline
PECAM	platelet endothelial cell adhesion molecule
RIP	rat insulin promoter
Texas Red	Texas Red-Dextran 70 kDa
3D	three dimensional
TPLSM	two-photon laser-scanning microscopy
YC-3.0	yellow chameleon 3.0
WHO	world health organization

1 INTRODUCTION

Insulin is the only blood glucose lowering hormone and thereby a key regulator of glucose homeostasis. The release of insulin from the pancreatic β-cell is regulated by a sophisticated interplay between nutrients, hormones and neurotransmitters. Diabetes mellitus is a disease state characterized by disturbed glucose homeostasis due to the insufficiency or lack of insulin. Type 1 diabetes is caused by an autoimmune reaction involving destruction of β-cells resulting in absolute lack of insulin secretion (1). Type 2 diabetes is characterized by β-cell dysfunction and thereby inability to secrete enough insulin to compensate for the increased need for insulin due to insulin resistance (2; 3). The world health organization (WHO) estimates that diabetes today affects 180 million people worldwide, of which 10% have type 1 diabetes (4).

Recently, pancreatic islet transplantation has emerged as a potential treatment of type 1 diabetes (5; 6). Transplanted islets have the capacity to restore endogenous insulin release and thereby glucose homeostasis. However, almost every patient requires islets from multiple donors and islet grafts have poor long-term function and survival (7). Today, there is a lack of methods to monitor β-cell function *in vivo*, which complicates our understanding of the mechanisms behind deterioration of islet graft function and β-cell mass (8). Isolation of islets from the pancreas disrupts the vascular connections and the delivery of oxygen and nutrients to the islet cells. Revascularization is therefore of vital importance for the survival and function of transplanted islets. Transplanted islets recruit blood vessels from the recipient organ (9; 10), although the newly established vascular network has low vessel density and impaired blood flow (9). Recent data suggests that donor islet endothelial cells (DIECs) might have the capacity to contribute to the revascularization of transplanted islets (11). Interventions that improve the revascularization of transplanted islets are likely to improve the survival and function of the endocrine cells.

Fluorescence microscopy has been successfully applied for studies of β-cell signal-transduction under *in vitro* conditions in cell and islet preparations, and have contributed novel information about β-cell physiology (12; 13). The application of laser-scanning microscopy (LSM) has facilitated functional studies of cells and blood vessels with high spatial and temporal resolution in living animals, and thereby significantly contributed to several fields of research (14-16).

The general aim of the work within this thesis was to develop and apply new experimental methods that facilitate functional studies of islet cells and islet revascularization under *in vivo* conditions after pancreatic islet transplantation. Therefore, LSM was applied together with two different transplantation models; *ex vivo* imaging of islets transplanted under the kidney capsule, and non-invasive *in vivo* imaging of islets transplanted to the anterior chamber of the eye. The results of this work introduce a novel platform for *in vivo* investigations of β-cell function and islet revascularization after islet transplantation.

1.1 THE PANCREATIC ISLETS

The endocrine cells of the pancreas are the β-, α-, δ- and PP-cells, whose main role is to secrete hormones that regulate the blood glucose level. Insulin released by β-cells decreases blood glucose whereas glucagon released by α-cells has a counteractive effect and increases blood glucose. Somatostatin released by δ-cells inhibits the

secretion of both insulin and glucagon (17), whereas the function of pancreatic polypeptide released by PP-cells largely remains unknown. The endocrine cells are located within the pancreatic islets, also called the islets of Langerhans, which are structurally defined cell aggregates of 2000-5000 cells and constitute microorgans of 50-500 μm in diameter. Pancreatic islets are dispersed among the exocrine tissue and constitute 2% of the pancreatic volume (18). The cellular and structural arrangements within the islets provide a unique microenvironment for the endocrine cells. The close arrangement of islet cells enables intercellular coupling and paracrine interactions (17; 19; 20). The intraislet organization of endocrine cells varies among species. In rodents, the islet core is primarily composed of β-cells while the other cell types are localized peripherally (21). In man, the distribution of the different endocrine cells is heterogeneous and no anatomical pattern of organization is obvious (22; 23). How the architectural differences among islets from different species affects the function of islet cells is currently not known (23).

Pancreatic islets are interspersed by a dense and tortuous vasculature that is different from the vasculature of the exocrine pancreas (24). The islet blood flow is regulated separately from the exocrine tissue and is five times higher (25). High blood flow provides efficient delivery of oxygen and nutrients to the islet cells. Furthermore, the islet blood flow increases in response to rising glucose levels (26; 27). The intraislet endothelial cells (ECs) are very thin, less then 100 nm, have a large number of fenestrations, small pores, and are lined with a thin layer of extra cellular matrix (24). Altogether, this arrangement creates a close distance, less then 500 nm, between the blood stream and the islet cells, which allows for a rapid transport of glucose and insulin between blood and β-cells (24). Recent data also suggest that there is continuous dynamic intercommunication between endocrine cells and intraislet ECs. Intraislet ECs produce extracellular matrix proteins that affect insulin gene expression (28; 29). In addition, blockade of islet cell secreted vascular endothelial growth factor-A (VEGF-A) causes regression of fenestrations and blood vessels in the islet vasculature (30). Pathophysiological alterations in the islet vasculature have recently also been observed to precede the rise in blood glucose levels in a model of type 2 diabetes (31).

Abundant innervation from both the parasymphatic and symphatic systems are present in the pancreatic islets (32). Several neurotransmitters and neuropeptides reside within these nerve endings and further contribute to the unique islet microenvironment (32; 33).

1.2 THE PANCREATIC β-CELL

The pancreatic β-cell acts as a metabolic sensor and secretes insulin to counteract rising levels of blood glucose. The release of insulin from the pancreatic β-cell is regulated by a sophisticated interplay between nutrients, hormones and neurotransmitters. The entry of glucose into the β-cell triggers an intracellular cascade of signaling events that leads to insulin release, which is referred to as the stimulus-secretion coupling (Figure 1). Briefly, glucose is taken up into the β-cell by a high capacity glucose transporter (GLUT), which ensures rapid equilibration between the intra- and extracellular glucose concentrations. Inside the cell, glucose is phosphorylated to glucose-6-phosphate by glucokinase (34) before entering glycolysis and the Krebs cycle. The metabolism of

glucose generates ATP and an elevation of the ATP/ADP ratio, which leads to closure of ATP-sensitive K^+ channels and resulting depolarization of the β-cell plasma membrane. As a consequence, opening of voltage-gated L-type Ca^{2+} channels leads to an increase in the cytoplasmic free Ca^{2+} concentration ($[Ca^{2+}]_i$), which promotes the release of insulin containing vesicles (35-37). In addition to glucose and other nutrients, a plethora of signaling molecules have been shown to affect the intracellular signaling cascade in the β-cell and thereby the biosynthesis and release of insulin. These effects have been attributed to hormones (17; 38), free fatty acids (39; 40), neurotransmitters (32; 41), neuropeptides (33; 41), paracrine mediators (42; 43), as well as to the autocrine feedback of insulin itself (44; 45).

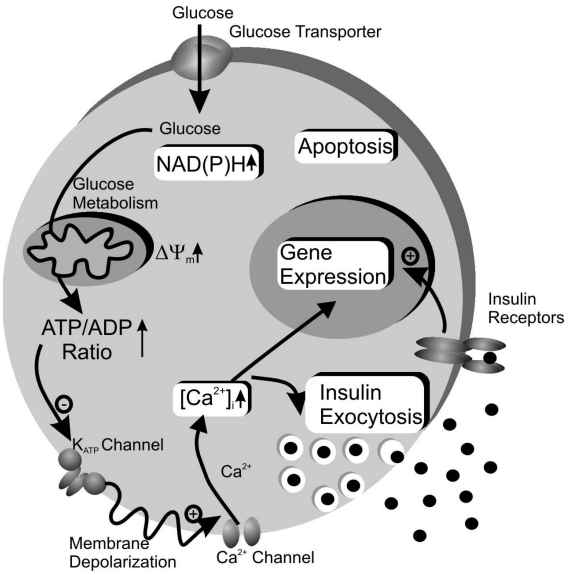

Figure 1. Key steps of the stimulus-secretion coupling in the β-cell. Steps highlighted in boxes are cellular events that can be monitored with fluorescent reporters in living β-cells and have facilitated, or have potential to facilitate, *in vivo* imaging of β-cell physiology. Illustration by Dr Tilo Moede.

Under physiological conditions in the body the release of insulin is the final result of a multitude of inputs that are integrated through intracellular events in the β-cell. Therefore, in order to understand how the release of insulin is regulated, β-cell signal-transduction needs to be investigated under *in vivo* conditions. However, the dispersed localization of islets within the pancreas makes β-cells difficult to access, and thus *in vivo* studies of β-cell signal-transduction have so far been limited in number and restricted to measurements of electrical activity (46; 47), and whole islet $[Ca^{2+}]_i$ imaging (48).

1.3 ISLET TRANSPLANTATION

Today, type 1 diabetes is treated with life-long insulin replacement therapy. This is an imperfect treatment associated with development of diabetes related complications and increased mortality. Recently, a breakthrough in clinical islet transplantation was

achieved with the establishment of the "Edmonton Protocol", which reported 80% success rate one year after transplantation (6). Follow-up studies have shown that transplanted islets possess the capability to restore endogenous insulin release and glucose homeostasis over long time-periods in persons with type 1 diabetes (7). As a consequence, islet transplantations are today performed in clinics around the world (5). Despite promising progress, several problems need to be addressed before islet transplantation can be offered to a large number of type 1 diabetics (7). To date, a large quantity of islets, around 12,000 islet equivalents/kg, are transplanted to each recipient through multiple isolation and transplantation procedures (7). Large number of islets appears to be destroyed during the transplantation procedure when the islets come in contact with blood. This occurs through an instant blood-mediated inflammatory reaction (49; 50). However, also after the engraftment of transplanted islets, continuous loss of β-cell function is evident by declining levels of released insulin (7). In the clinical setting, evaluation of islet graft function is restricted to hormone secretion assays, and no method currently exists to determine the mass of engrafted islets. Consequently, it becomes very difficult to determine the number of surviving islets after transplantation and their degree of functionality, which makes it very complex to elucidate the mechanisms that underlie deterioration of islet graft function (8).

In the experimental setting, the first successful islet transplantation that cured diabetes was reported in 1972 (51). However, as in the clinical setting, alternatives to monitor islet mass and β-cell function *in vivo* after transplantation are limited. Developments within magnetic resonance imaging (MRI) (52), positron emission tomography (PET) (53) and bioluminescence optical imaging (54; 55), have recently been reported which demonstrate the feasibility of monitoring islet mass *in vivo* following transplantation. Monitoring of islet mass in combination with hormone secretion assays will provide more information about the relationship about the number of surviving islets and their functionality (56). However, the current resolution and application of these techniques do not allow studies of cellular morphology or signal-transduction.

1.4 ISLET REVASCULARIZATION AFTER TRANSPLANTATION

The procedure of islet isolation disrupts all vascular connections and leaves the islets dependent on diffusion for the delivery of oxygen and nutrients. Consequently, there is a risk for the development of hypoxia in isolated islets, which may result in cell death (57). After transplantation the islets are engrafted, i.e. adapted to the transplantation-site, in a process characterized by structural rearrangements of the tissue, revascularization and reinnervation (9). Immediately after transplantation, islet cells suffer from hypoxia, dramatic reduction in insulin contents and high incidents of cell death (58; 59). As the growth of vessels into the islets starts and the revascularization progresses, the levels of cell death and hypoxia decrease, and the insulin content increases (58).

Transplanted islets recruit new blood vessels in a process that has been reported to be completed within ten to twenty days after transplantation (60-62). The islet graft vasculature is established by vessels that grow into the transplanted islets from the recipient organ (63). Islets with reduced secretion of VEGF-A recruit less vessels after transplantation compared to control islets, indicating an important role for islet cell secreted VEGF-A in the revascularization process (64). Circulating endothelial precursor cells have also been suggested to contribute to vessel formation (65). In

addition to recipient derived vessels, donor islet endothelial cells (DIECs) have the capacity to participate in vessel formation and to contribute to revascularization of transplanted islets (11; 66; 67), see chapter 4.2. The established islet graft vasculature has low vessel density (68) compared to islets localized *in situ* in the pancreas. The low vessel density has been associated with impaired functionality of islet grafts, such as reduced blood flow (9; 69) and low oxygen tension (70; 71), when compared to islets in the pancreas.

Due to the high rates of cell death during the immediate post transplantation period, and because of the low vessel density in islet grafts, different strategies to improve the revascularization of transplanted islets have been evaluated. Different angiogenic growth factors have been applied locally on the tissue at the transplantation-site prior to the transplantation of islets to attract vessels and achieve a pre-vascularization. Results from this strategy has reported improved revascularization rate (72), and increased capacity of transplanted islets to reverse diabetes (73). VEGF-A has been overexpressed in islet cells to improve the angiogenic capacity of the islets (74-76). Transplantation of islets that overexpress VEGF-A increases vascular density of the islet grafts (74; 75). In addition, the islet grafts had increased blood flow (75) and insulin content (74), as well as an improved capacity to reverse diabetes (74; 75). Complementary to these results, systemic blockade of angiogenesis during the fourteen first days post islet transplantation results in decreased vascularization of islet grafts, which is associated with reduced insulin content and islet mass, as well as an inability of the transplanted islets to reverse diabetes (77). Treatment of mice with the clinically used immunosuppressive drug rapamycin reduces the revascularization of transplanted islets (78; 79). Rapamycin treatment also results in decreased insulin content and insulin secretion from islet grafts (78). In summary, these results indicate that the revascularization of transplanted islets is strongly linked to the survival and function of islet grafts. Thus, interventions that improve revascularization of transplanted islets are likely to improve the survival and function of the endocrine cells.

1.5 *IN VIVO* FLUORESCENCE IMAGING

Fluorescence microscopy is today applied together with a wide array of fluorescent reporters for investigations of a multitude of different cell physiological parameters under different conditions. The focus of the work within this thesis has been to apply fluorescence imaging for cellular studies under *in vivo* conditions. This chapter will therefore introduce LSM and fluorescent reporters that have been applied, or have a potential application, to studies of islet cells or vasculature within living animals.

1.5.1 Laser-scanning microscopy (LSM)

Confocal laser-scanning microscopy (confocal microscopy) and two-photon laser-scanning microscopy (TPLSM) (80) are two fluorescence imaging techniques that enable images to be captured from the fluorescence signal of the focal plane only. This gives a great advantage for imaging in multilayer tissues compared to widefield fluorescence microscopy, where the fluorescence signal from the focal plane is highly contaminated by signals from above and below that focal plane (81). The ability to capture an optical section from the focal plane only, without contribution of out-of-focus light, allows for optical sectioning within a multilayer tissue (81). Practically, a stack of images can be collected with high spatial resolution at different focal depths, which permits three dimensional (3D) reconstruction by computationally combining the

image data from the stack of images (81). Optical sectioning can also be applied in a temporal mode to collect image series from one focal plane inside a multi-cellular tissue, which is useful for studies of signal-transduction. By collecting image stacks in a temporal mode, four dimensional (4D) data can be generated of the specimen (82).

Confocal microscopy and TPLSM can be applied in the same microscope, although different lasers and detectors are required. With confocal microscopy the specimen is illuminated with a continuous laser beam, which causes the entire specimen thickness to fluoresce. The out-of-focus light from areas above and below the focal plane is rejected in front of the detector by a pinhole (81). This arrangement brings some drawbacks for imaging within multilayer tissues. Although the collected fluorescence only originates from one focal plane, the laser-light induces bleaching and photodamage in the tissue that is localized above and below the focal plane. In addition, the pinhole does not only reject photons from out-of-focus planes, but also photons derived from the focal plane that have been scattered on their way to the detector (83). TPLSM uses a pulsed laser beam that send ~80 million pulses per second, each pulse has a duration of ~100 fs (84). These pulse trains are needed to facilitate excitation by two-photon absorption, which means that two photons which arrive simultaneously (within ~0.5 fs) combine their energies for excitation of the fluorophore (83). To generate multiphoton absorption the excitation light has to be concentrated in space and time, which practically means that excitation only occurs in the focal plane. Since TPLSM only generates excitation in the focal plane, no bleaching or photodamage is generated above or below the focal plane. In addition, since all fluorescence is derived from the focal plane, no pinhole is needed and all emitted light can be collected, including scattered photons, which also results in less laser power requirements. Furthermore, because the energy of two-photons is used for excitation, excitation light with less energy and wavelengths in the near-infrared range (700-1000 nm) is used. Near-infrared light penetrates deeper into tissue and generates less photodamage due to the lack of endogenous absorbers (83). As a result, TPLSM can be used to image deeper in tissue than confocal microscopy. TPLSM imaging has been reported at a depth of 1 mm in living brain (85). However, the scattering properties of the tissue and the properties of the applied fluorophore determine the possible imaging depth.

1.5.2 Fluorescent reporters for β-cell signal transduction

LSM has together with different fluorescent reporters facilitated imaging of signal-transduction in β-cells under *in vitro* conditions in isolated islets and cells (12; 13). Many of these reporters could potentially be applied for *in vivo* imaging and will be briefly mentioned together with the signaling events that are highlighted in Figure 1. The cloning and the first use of GFP as an intracellular reporter in living cells (86) and transgenic mice (87) laid the foundation for today's extensive use of fluorescent proteins as intracellular reporters (88-90). By using the insulin promoter, the expression of fluorescent reporter proteins can be directed to the β-cell (91; 92). Successful introduction of fluorescent reporter constructs into pancreatic islet cells has been achieved by viral transduction (93-95) and the creation of transgenic mice (92; 96). This has established the platform for the use of fluorescent reporter proteins for *in vivo* imaging of islet cells.

The rat insulin promoter (RIP) has been used to report the regulation of insulin gene expression by driving expression of GFP (91). By driving the expression of the

red fluorescent protein DsRed with another promoter of interest, the regulation of multiple promoters can be simultaneously studied in individual β-cells (95). Glucose metabolism has been successfully monitored in pancreatic islets by TPLSM imaging of the intrinsic autofluorescence of NAD(P)H (97). The possibility to use autofluorescence of endogenous NAD(P)H circumvents problems with transgenic expression or loading, although the signal to noise ratio is low and sensitive to photodamage. Ca^{2+} is an important second messenger and plays a key role in the stimulus-secretion coupling in the β-cell. A multitude of genetically encoded (98) and chemical Ca^{2+} indicators have been developed and applied in living cells and animals. To date, the use of genetically encoded Ca^{2+} indicators has been limited in β-cell research (96; 99; 100). The current development of the genetically encoded Ca^{2+} indicators (101; 102) continuously improves their qualities as Ca^{2+} reporters and make them a promising future approach for monitoring of β-cell function *in vivo*. *In vivo* Ca^{2+} imaging in the brain has successfully been performed by introducing chemical probes with micropipettes (103), or by bulk loading (104). Similar approaches could be potentially interesting for islet cells, although the introduction of Ca^{2+} probes *in vitro* only results in loading of the most superficial cell layers in islets (12; 100). Imaging of insulin secretion have been facilitated in β-cells by using a pH-sensitive variant of GFP (105). Interestingly, a similar reporter construct has enabled *in vivo* imaging of secretion from neuronal cells in transgenic mice (106). Creation of reporter mice that express this reporter construct in β-cells may constitute a methodological approach for *in vivo* monitoring of insulin release. Apoptosis has been visualized in insulin producing cells by a reporter construct that uses fluorescence resonance energy transfer (FRET) to specifically report caspase activity (107). Annexin V conjugated to a near-infrared probe has also been used to detect β-cell apoptosis. By systemic injections and *ex vivo* imaging of the excised pancreas, annexin V was shown to specifically label pancreatic islets (108). Real-time imaging of annexin V labeling of dying cells in a model of heart ischemia has also been achieved (109).

1.5.3 Imaging of blood vessels and transplanted cells

The ability to generate fluorescent cells has greatly facilitated the identification and tracking of transplanted cells and has been used in a variety of applications. The application of *in vivo* fluorescence imaging of transplanted islets has so far been limited. By insertion of a body-window, pancreatic islets transplanted under the kidney capsule were visualized by a GFP variant expressed in β-cells in combination with labeled lymphocytes (110). The application of a body-window has enabled several studies of islet revascularization after islet transplantation to the dorsal skinfold chamber preparations in hamsters and mice. In this model, the transplanted islets engraft on the skin muscle and are imaged with widefield microscopy through a coverslip mounted in a titanium frame (61; 111). By using this preparation, studies of vessel properties and blood flow have been performed (60; 61; 112). Imaging of islet revascularization of islets transplanted under the kidney capsule has also been achieved by *in vivo* confocal microscopy in rats (62; 113).

2 AIMS

The overall objective of this thesis was to develop and apply experimental models that facilitate functional studies of islet cells and islet revascularization after pancreatic islet transplantation under *in vivo* conditions by the use of fluorescence imaging techniques. The specific aims were:

1. To characterize fluorescent reporter protein expression and the physiology of a transgenic mouse model, with special emphasis on the pancreatic islets.

2. To investigate how intraislet ECs are affected by islet isolation and islet culture, and additionally if intraislet ECs participate in blood vessel formation after transplantation.

3. To characterize the contribution and the effect of DIECs on the revascularization of islets after transplantation.

4. To establish an experimental platform for *in vivo* fluorescence imaging of β-cell function and islet revascularization.

3 MATERIALS AND METHODS

3.1 MATERIALS

Materials used in the experiments reported in this work are described in detail in the papers (I-IV).

3.2 MOUSE MODELS

Tie2-GFP mice (STOCK Tg(TIE2GFP)287Sato/J) were purchased from the Jackson Laboratories (Bar Harbor, ME). YC-3.0 transgenic mice were kindly donated by professor R.Y. Tsien at the University of California and have previously been described (114). C57BL/6, C57BL/6 nude mice (B6;Cg/JBomTac-Foxn1^{nu}N3) and NMRI nude mice (NMRI-*Foxn1^{nu}*) were purchased from Taconic M&B (Ry, Denmark). RIP-GFP mice were generated by injections of the RIP1.EGFP expression cassette into one-cell stage embryos from B6CBAF1/Crl donors. The obtained F0 generation was scored for RIP1.EGFP genomic integration by PCR analysis. The RIP1.EGFP transgene was observed in seven potential transgenic founders (17.5%), which were mated with inbred C57Bl/6NCrl mice to generate F1 animals. The founder lines were screened with regards to 1) the expression of GFP in β-cells as determined by immunostaining, and 2) animal and cell physiology. The RIP1.EGFP founder line #29 was found to have normal glucose tolerance when compared to control animals and β-cell restricted expression of GFP, and was selected for homozygote breeding.

3.3 PANCREATIC ISLETS

3.3.1 Isolation and islet culture

For pancreatic islet isolation, mice were starved overnight and killed. The abdominal side was opened up and 4-5 ml of 2 mg/ml of collagenase was injected into the pancreas via the bile duct. The distended pancreas was removed and kept on ice for maximum 1 h before digestion at 37°C. Following digestion the pancreas was dissociated and washed with cold Hanks' Balanced Salt Solution before islets were purified using a discontinuous gradient of Histopaque 1077 and 1119, followed by handpicking. Islets were cultured in suspension in RPMI 1640 medium supplemented with 10% fetal calf serum (FCS), 2 mM L-glutamine, 100 IU/ml penicillin and 100 μg/ml streptomycin. The culture medium was changed every second day. In paper II, the culture medium was supplemented with either endothelial cell growth supplement (ECGS) at a final concentration of 100 μg/ml, or both fibroblast growth factor (FGF) and VEGF at final concentrations of 20 ng/ml and 10 ng/ml, respectively.

3.3.2 Glucose-stimulated insulin release

Groups of ten islets were transferred in triplicate to glass vials containing 250 μl Krebs-Ringer bicarbonate buffer supplemented with 10 mM HEPES and 2 mg/ml bovine serum albumin (hereafter referred to as KRBH buffer). The KRBH buffer contained 1.67 mM D-glucose during the first hour of incubation at 37°C. The medium was removed and replaced by 250 μl KRBH supplemented with 16.7 mM glucose and incubated for a second hour. After retrieval of the media, the islets were harvested, pooled in groups of 30, and homogenized by sonication in 200 μl redistilled water. Two 50 μl aliquots of the aqueous homogenate were used for DNA measurements by fluorophotometry (115). A fraction of the homogenate was mixed with acid-ethanol

(0.18 M HCl in 95 % ethanol) from which insulin was extracted overnight at 4°C. Insulin concentrations in incubation media and homogenates were determined by a commercial mouse insulin ELISA (Mercodia).

3.3.3 Glucose oxidation rate

Islet glucose oxidation rates were determined according to a previously described method at the department of Medical Cell Biology, Uppsala University (116).

3.4 ANIMAL FLUORESCENCE AND PHYSIOLOGY

3.4.1 EYFP fluorescence in tissues

For studies of whole animal fluorescence, animals were sacrificed and the skin together with the underlying muscle layer was removed from the abdominal side. Pictures of whole animal fluorescence were captured using a cooled CCD camera (Astrocam) connected to a Leica MZFLIII stereomicroscope with filters for EYFP fluorescence. Using the described equipment and living animals under isoflurane anesthesia, EYFP fluorescence from transplanted YC-3.0 islets under the kidney capsule was visualized.

3.4.2 Pancreas perfusion

The pancreas perfusions were performed at the department of Medical Cell Biology, Uppsala University as previously described (117).

3.4.3 Blood flow measurements

The blood flow measurements were performed at the department of Medical Cell Biology, Uppsala University as previously described in detail (118; 119).

3.4.4 Induction of β-cell death

Tie2-GFP mice transplanted with RIP-GFP islets to the anterior chamber of the eye and male C57BL/6 nude mice were injected intravenously with the β-cell toxic agent alloxan (80 mg/kg body weight) (120), which is taken up into β-cells by GLUT2. Blood glucose concentrations were measured one week after injections in C57BL/6 nude mice and animals exceeding 18 mmol/l were considered diabetic. Blood glucose concentrations were measured in Tie2-GFP mice one day after injections.

3.5 PANCREATIC ISLET TRANSPLANTATION

3.5.1 Transplantation under the kidney capsule

The recipient animal was anesthetized using isoflurane. An incision was made through the skin and the underlying muscle layer, before the left kidney was carefully extracted out of the body cavity. A small cut was made through the kidney capsule and 200-400 islets were placed in a pocket just under the capsule. The kidney was gently inserted back into the body cavity and the animal was sutured. Temgesic was administered to relieve post-operative pain.

3.5.2 Transplantation to the anterior chamber of the eye

Around 30 islets were transferred from culture media to sterile phosphate buffered saline (PBS) before aspirated up into a 27G eye cannula connected to a 1 ml Hamilton syringe via a 0.4 mm polythene tubing. The mouse was anesthetized using isoflurane and Temgesic was administered to relieve post-operative pain. Under a stereomicroscope, the cornea was punctured close to the sclera at the bottom part of the eye with a 27G needle. Great care was taken not to damage the iris and to avoid bleeding. Next, the blunt eye cannula was gently inserted and the islets were slowly injected into the anterior chamber where they settled on the iris. After injection, the cannula was carefully withdrawn and the animal was left lying on the side before awakening. The transplanted mice quickly recovered and showed no signs of stress or irritation from the transplanted eye.

3.6 FLUORESCENCE IMAGING

3.6.1 Microscope set up and imaging settings

A Leica TCS-SP2-AOBS confocal laser-scanner equipped with Argon and HeNe lasers connected to a Leica DMLFSA microscope was used for all imaging applications in combination with different objectives. Two-photon excitation was achieved using a Ti:Sapphire laser (Tsunami; Spectra-Physics, Mountain View, CA) for ~100 fs excitation at ~82 MHz. The excitation wavelengths and detector settings for collection of emission light for the different fluorophores are listed in Table 1.

Fluorophore	**Excitation (nm)**		**Emission (nm)**	
	1P	**2P**	**1P**	**2P**
GFP	488	890	495-525	BP 525/50
fluorescein isothiocyanate (FITC)	488	890	495-525	BP 525/50
Texas Red		890		BP 640/20
EYFP	514		518-560	
Allophycocyanin (APC)	633		644-680	
Alexa Fluor 488	488		495-525	
Alexa Fluor 546	543		550-600	
Alexa Fluor 633	633		645-680	

Table 1. Fluorophores with 1- respective 2-photon excitation wavelengths and detector settings for collection of emission light.

3.6.2 Imaging of reflection light

Reflected light was used to localize and visualize pancreatic islet cells after transplantation. Since the pancreatic endocrine cells are densely packed with hormone containing vesicles they reflect light to a high extent, other tissue structures also reflect light but usually to a much lower extent. Technically, reflected light was captured by confocal imaging, usually by illumination at 633 nm and collection of reflected light between 630-635 nm, with the acousto optical beam splitter (AOBS) set to optimal reflection mode.

3.6.3 Imaging of intact Tie2-GFP islets

For imaging, individual islets were transferred from culture medium to PBS and the intact islet was imaged with TPLSM using a dipping objective (40x). Image z-stacks, starting at the uppermost detectable fluorescence of the islet and ending when the GFP fluorescence signal from the islet center was lost, were captured. Every image was captured with a one-micron step interval and the stacks usually corresponded to physical distance of ~60 μm. Before the image analysis was performed, bright spots of non-GFP fluorescence appearing in both the GFP and the Texas Red channel were removed from the GFP channel by subtracting with the fluorescence from the Texas Red channel.

3.6.4 *Ex vivo* imaging of kidney islet grafts

The perfusion of graft-bearing kidneys were modified from Korsgren et al (121). At the time-point for imaging, the mouse was anesthetized with isoflurane and placed on a heating pad. The abdominal cavity was cut open and the left kidney together with the aorta and the caval vein were made visible by moving the overlaying organs to the side and wrapping them in moist compresses. The left kidney together with the aorta and the caval vein were carefully prepared free from surrounding tissue. Thereafter, the branching vessels in the regions above and below the renal vessels were electrically coagulated and cut. The aorta and the right renal vessels were ligated with a thread above the branch of the left renal vessels. The lower part of the aorta was cut and cannulated with a thin plastic catheter connected to a running perfusion system. Subsequently the vena cava was cut open and cannulated with a plastic catheter. The catheters, acting as in- and outlet for the perfusion buffer, were kept in place with two threads. The kidney preparation was then cut free from the aorta and the vena cava before it was transferred to a custom made chamber and placed on soft and moist compresses. A coverslip was carefully placed on top of the kidney, covering the region of the islet graft. Finally, the chamber was attached to the microscope stage and kept at 37°C. The time from induction of anesthesia to the start of imaging was approximately 30 min. The kidney preparation was constantly perfused with a buffer containing in mM, 118.5 NaCl, 4.7 KCl, 1.2 KH_2PO_4, 25.0 $NaHCO_3$, 2.5 $CaCl_2$, 1.2 $MgSO_4$, 5 HEPES, 3 glucose and 2 mg/ml of BSA. The buffer was equilibrated to pH 7.4, by gassing with 95/5% O_2/CO_2 gas, before it was loaded into a pressure regulated multi-channel perfusion system. The O_2/CO_2 gas was used to pressurize the perfusion system and to set the flow rate at 200-300 μl/min. Texas Red-Dextran 70 kDa (Texas Red) was added utilizing a syringe pump, as indicated during continuous perfusion.

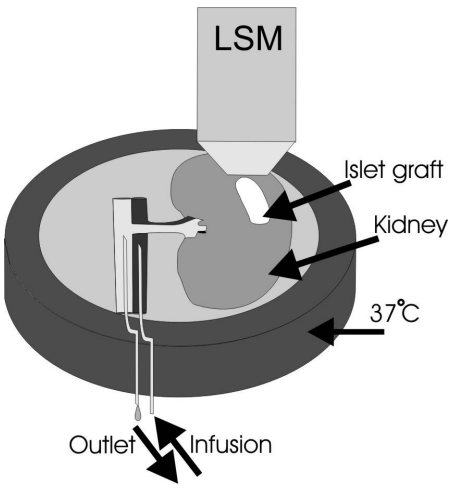

Figure 2. Illustration of the *ex vivo* set up.

Ex vivo imaging was conducted with confocal and TPLSM. Using 10-20x magnifying lenses the islet grafts could be easily distinguished under the kidney capsule and images that covered large surface areas (1.2 x 1.2 mm) could be captured. For image z-stacks, series of images were captured with 1-3 micron distance in

between each image. During the imaging of time-sequences, continuous scanning was applied and one image was scanned approximately every third second.

3.6.5 *In vivo* imaging of islets engrafted in the anterior chamber of the eye

The transplanted mouse was anesthetized with 40% oxygen and ~2% isoflurane mixture, placed on a heating pad and the head was restrained with a stereotaxic headholder. The head was positioned with the transplanted eye facing up. The eyelid around the right eye was carefully pulled back and the eye was gently held at the corneoscleral junction with a pair of tweezers attached to a micromanipulator (Narishige). This arrangement permitted a flexible but stable fixation of the head and eye without causing damage or disrupting the circulation of the eye.

In vivo imaging was conducted with both confocal and TPLSM using long-working distance dipping lenses with filtered saline as immersion liquid. For visualization of blood vessels, Texas Red (100 µl, 10 mg/ml) was intravenously injected via the tail vein. Texas Red reached the vasculature of the engrafted islets within 10 s after injection. For visualization of cell death, 100 µl of annexin V-APC was intravenously injected via the tail vein. The transplanted islets were imaged 4-6 h following the administration of annexin V-APC.

3.7 IMMUNOHISTOCHEMISTRY AND IMMUNOSTAINING

3.7.1 Pancreas, islets and kidney islet grafts

Isolated islets were fixed in 4% paraformaldehyde for 15 min at 8°C. After fixation, islets were washed in PBS, incubated for 45 min in a 15% sucrose-PBS solution at 4°C. Pieces of pancreas or cut out kidney islet grafts were fixed for 3-4 h in 4% paraformaldehyde at 4°C. Thereafter, washed in PBS, incubated first in a 15%, and then in a 30%, sucrose-PBS solution at 4°C. After sucrose substitution, all tissues were embedded in Tissue-Tek O.C.T. Compound, frozen and stored at -80°C. Ten-micrometer thick sections of both islets and islet grafts were cut using a cryostat and adhered to glass slides. The sections were washed with OptiMax Wash Buffer, which was used for all subsequent washings, before blocking with goat serum for 20 min and application of primary antibodies for 1 h. A ready-to-use polyclonal guinea pig anti-insulin antibody (Biogenex) or a polyclonal guinea pig anti-insulin antibody (Biogenex) at 1:100 dilutions was used for insulin detection. A monoclonal rat anti-mouse CD31, also known as platelet endothelial cell adhesion molecule (PECAM), antibody (BD Bioscience Pharmingen) at 1:50 dilution was used for CD31 detection (122). A rabbit polyclonal anti-GFP antibody (Molecular Probes) at 1:100 dilutions was used for GFP detection (paper II). The sections were washed before secondary antibodies anti-rabbit Alexa Fluor 488, anti-guinea pig Alexa Fluor 546 or 633, and anti-rat Alexa Fluor 633 were applied for 20 min at 1:200 dilutions. The sections were washed before mounted with coverslips using ProLong Antifade Gold. Confocal image z-stacks were captured of the tissue sections, starting and ending at the uppermost respectively the lowermost detectable level of fluorescence. Multiple fluorophores were imaged sequentially to eliminate spectral overlaps.

3.7.2 Anterior chamber engrafted islets

Eyes were removed and fixed in 4% paraformaldehyde for 1 h. After cryoprotection by substitution in 10%, 20%, and 30% sucrose in PBS the eyes were frozen at -80°C.

Fourteen micrometer thick vertical sections of the eyes were cut on a cryostat. Sections were washed in PBS before incubated in PBS containing 5% bovine serum albumin and 0.1% triton for 1 h. Thereafter, sections were incubated overnight in PBS with primary antibodies; anti-insulin 1:500 (Accurate Chemical & Scientific Corp.) and anti-glucagon 1:5000 (Sigma). Immunostaining was visualized using either Alexa 488 or Alexa 568 conjugated secondary antibodies at 1:500 dilutions. Cell nuclei were stained with 4',6-diamidino-2-phenylindole (DAPI) and slides were mounted with Vectamount and coverslipped.

3.8 IMAGE ANALYSIS AND QUANTIFICATION

3.8.1 Vascular density in isolated Tie2-GFP islets

The vascular density was defined as the number of blood vessels, i.e. distinct regions of ECs, per tissue area. In the intact islets scanned with TPLSM, the vascular density was calculated from GFP fluorescent cells. The vascular density of each islet was determined as the mean value of the vascular density calculated in three different optical sections captured at 15, 30 and 45 μm depth in the islet. In the islet sections, the vascular density was calculated from the combined GFP and CD31 staining in image projections. The values obtained for the vascular density with each method were normalized by dividing with the values obtained at Day 0.

3.8.2 DIECs contribution and total vessel area in kidney islet grafts

To determine the contribution of DIECs to the vasculature and the total vessel area of kidney islet grafts, the area of GFP and CD31 fluorescence were quantified in immunostained kidney islet graft sections. The CD31 fluorescence corresponded to the total vasculature since CD31 label both host- and donor-derived ECs, whereas the GFP fluorescence corresponded to the DIECs. A difference in the level of vascular density has been reported between the stromal area (high) and the endocrine area (low) of kidney islet grafts (68; 123; 124). Therefore, we decided to quantify and present all parameters separately for these two areas from the kidney islet grafts. The fluorescence of the image stacks captured of the immunostained sections was normalized using the background fluorescence of non-labeled tissue as a reference. All images were then converted to a binary format and the GFP and CD31 fluorescence were quantified in three areas of the grafts. The endocrine area, as determined by insulin staining. The stromal area, defined as the entire graft above the kidney tubuli except the endocrine area. Non-vascularized islets, i.e. insulin-stained islet structures lacking a penetrating vasculature, but surrounded with a sheet of vessels. For each graft, an area of 0.6-1.6 mm^2 was analyzed, which was captured from 4-9 tissue sections selected over a 0.5 mm region of the graft.

3.8.3 Vessel density and diameter in anterior chamber engrafted islets

The vessel density and the vessel diameter of the islet graft vasculature were quantified after transplantation to the anterior chamber of the eye. The vessel density was determined as the number of vessel segments per graft area. A vessel segment was defined as a single vessel or a branch of a vessel. Two optical sections were quantified from each islet graft. The optical sections were selected from image series of z-stacks. The first section was selected at the deepest level in the graft, ~50-60 μm, without loss of signal. The second section was selected in the middle of the graft, between the surface and the deepest section. The quantification was made with the Leica Confocal Software (version 2.61).

3.8.4 Proportion of endocrine cells in anterior chamber engrafted islets

Serial cross sections of eyes containing islets were examined for the presence of insulin and glucagon. All immunostaining images were digitally acquired and recompiled (Photoshop 5.0). Sections were viewed at 10x and 40x magnification. Analyses were done on digitized fluorescence microscopic images using Zeiss Axiovision software. The ratio of insulin-immunoreactive cells / glucagon-immunoreactive cells were calculated as the average from at least three adjacent sections from at least two separate islets per eye. The results from three eyes were averaged. Only cells that had a clearly labeled nucleus (DAPI staining) were included in the analyses.

3.9 STATISTICAL ANALYSIS

All values are given as means ± SEM. Students unpaired *t*-test was used and $P<0.05$ was considered to be statistically significant for all comparisons.

4 RESULTS AND DISCUSSION

4.1 FUNCTIONAL CHARACTERIZATION OF THE YC-3.0 REPORTER MOUSE

The YC-3.0 reporter mouse is characterized by transgenic expression of the yellow chameleon 3.0 (YC-3.0) protein (125). Our aim was to investigate the transgenic expression in pancreatic islet cells and to perform a physiological characterization with focus on glucose homeostasis and pancreatic islet function in the YC-3.0 mouse. Fluorescence from the enhanced yellow fluorescent protein (EYFP), one part of the hybrid YC-3.0 protein, was used as a reporter for transgenic expression. The expression of the YC-3.0 protein is regulated by the β-actin promoter and the cytomegalovirus enhancer, which results in ubiquitous tissue expression that was evident in the YC-3.0 mouse (Paper I, Figure 1). The transgenic expression in different tissues varied, which has also previously been reported (114). Confocal imaging of sections from YC-3.0 pancreases showed that EYFP was expressed throughout all islets cells. EYFP expression in β-, α- and ECs was additionally confirmed by cell specific antibodies (Paper I, Figure 2). Confocal imaging of intact isolated YC-3.0 islets further confirmed that EYFP was expressed in all islet cells, and additionally displayed the distinguished intensity difference between autofluorescence in normal islets and EYFP fluorescence in YC-3.0 islets (Paper I, Figure 3). *In vivo* imaging of YC-3.0 islets transplanted under the kidney capsule of nude mice showed that EYFP fluorescence could be used to differentiate between donor islets and recipient tissue (Figure 3; Paper I, Figure 4).

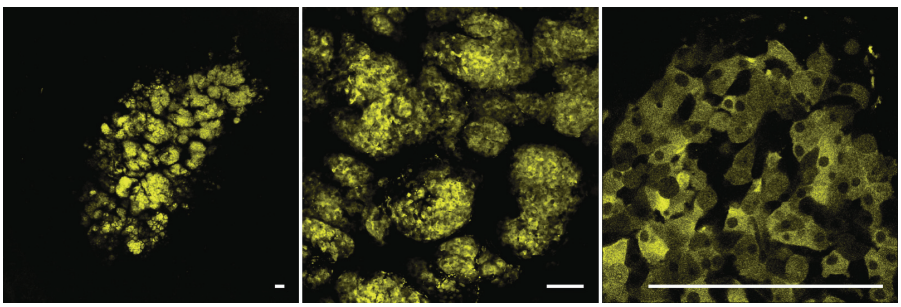

Figure 3. Fluorescence images of YC-3.0 islets transplanted under the kidney capsule. Three images captured from the same islet graft by *ex vivo* imaging display how the EYFP fluorescence can be used to identify transplanted donor islet cells when engrafted in non-fluorescent recipient tissue. Scale bars, 150 μm

Transgenic YC-3.0 mice were healthy and displayed similar organ morphology as control mice (Paper I, Table 1). Moreover, the morphology of the YC-3.0 pancreas was similar in terms of total weight, islet volume and islet mass. *In vitro* studies showed no difference in glucose induced insulin release from isolated islets or perfused pancreas of YC-3.0 and control mice (Paper I, Figure 5). Likewise, glucose handling was similar in YC-3.0 mice and control mice during intravenous glucose tolerance test (Paper I, Figure 6). Furthermore, transplantation of 400 YC-3.0 islets to alloxan-induced diabetic mice showed that YC-3.0 islets restored glucose homeostasis. Additionally, characterization of the circulation in YC-3.0 mice showed no difference in blood pressure or blood flow compared to control mice (Paper I, Table 1).

In conclusion, the transgenic YC-3.0 mouse displays a normal physiology with appropriate glucose homeostasis and pancreatic islet function. Fluorescent YC-3.0 islets open up new approaches for studies of engrafted islets following islet transplantation. As a proof of concept, transplantation of fluorescent YC-3.0 islets has facilitated identification and morphological investigations of islets transplanted to the liver (126), and isolation of islets transplanted both to liver and pancreas (127). The YC-3.0 mouse together with the different β-cell specific fluorescence reporter mice (92; 96), validate the expression of fluorescent reporters as a feasible methodological approach to facilitate studies of islet cell physiology.

4.2 DIECS IN ISLET REVASCULARIZATION AFTER TRANSPLANTATION

Revascularization and the re-establishment of blood flow is vital for the function and survival of transplanted islets. Until recently, transplanted islets were believed to solely become revascularized by the ingrowth of blood vessels from the recipient organ (10; 63). Using the transgenic Tie2-lacZ reporter mouse, Linn et al. (11) reported that DIECs could be found in islet grafts after islet transplantation. Together with the reported vascular impairment of islet grafts, this encouraged us to investigate the functional role of DIECs in revascularization of transplanted islets.

4.2.1 Intraislet ECs after islet isolation and islet culture

To investigate if intraislet ECs persist after islet isolation, pancreatic islets were isolated from Tie2-GFP mice. TPLSM imaging of intact Tie2-GFP islets directly after isolation showed that a large number of intraislet ECs remained in the islets and expressed GFP. This was confirmed by immunofluorescent staining of islet sections using antibodies against GFP and the EC marker CD31 (Paper II, Figure 1). All GFP expressing cells were found to express CD31, confirming an EC origin. When the expression of GFP and CD31 was compared, 81% of the CD31 expressing cells were found to express GFP. Thus, it was concluded that GFP is a relevant and useful reporter for intraislet ECs in Tie2-GFP islets. Recent data suggests that the expression of Tie2-GFP in the vasculature is asymmetric with little expression in venules (128). This suggests that the vessels in Tie2-GFP islets which express CD31 but not GFP could represent venules.

To investigate how islet culture affects intraislet ECs, Tie2-GFP islets were cultured under normal islet culture conditions, i.e. suspension culture in RPMI 1640 culture medium supplemented with 10% FCS. The intraislet ECs were quantified directly after isolation and during four consecutive days of culture by TPLSM imaging of intact islets. A rapid reduction in the number of intraislet ECs was observed during culture, and on the forth day of culture only 5% of the ECs remained compared to directly after isolation. This result was confirmed by immunostaining of islet sections, which additionally showed that the expression of GFP and CD31 decreased with similar rates during islet culture (Paper II, Figure 2). Linn et. al. (11) previously showed that intraislet ECs migrate out of islets and form cord-like structures when the islets are placed in a 3D matrix. Migration was stimulated by the addition of the growth factors VEGF and FGF (11). According to another report, cord-like structures was observed to extend from islets cultured in suspension when similar growth factors were added to the culture media (72). To investigate the effect of growth factors on intraislet ECs during islet culture, Tie2-GFP islets were cultured as described with a supplement of either

VEGF in combination with FGF, or a cocktail called ECGS (129). However, supplement of these EC growth factors did not affect the rapid loss of intraislet ECs during islet culture. Only a small increase in the number of ECs could be observed after four days of culture with supplement of VEGF and FGF, and no effect was observed after the addition of ECGS (Paper II, Figure 2). In summary, our data show that intraislet ECs persist in islets after islet isolation, but rapidly disappear during islet culture. Furthermore, the loss of intraislet ECs during islet culture was not affected by the addition of EC growth factors to the culture medium.

To date, intraislet ECs have been observed after islet isolation from several species, i.e. mouse (11; 67; 130; 131), rat (11; 129; 132), pig (11) and human (67; 75; 79; 133; 134). Together these reports show that intraislet ECs persist in islets after isolation independent of species and isolation technique. In accordance with our results, previous studies have shown that intraislet ECs are lost after seven days of culture of mouse (130) and rat islets (132). Furthermore, in line with our result, a recent study showed that addition of EC growth factors during islet culture does not affect the loss of intraislet ECs (131). Although the loss of intraislet ECs during islet culture has not been investigated in detail with markers for cell viability, it is likely that cell death plays a major role. However, dedifferentiation of ECs including the loss of expression of EC makers can not be excluded. Unfortunately, no current data exist on how human intraislet ECs are affected by islet culture.

Compiled data from several reports show that freshly isolated but not cultured islets contain intraislet ECs. Considering the tough period transplanted islets face before they are revascularized and the low vessel density in islet grafts, we questioned if intraislet ECs could participate and functionally contribute to the revascularization of transplanted islets. By transplanting freshly isolated islets with intraislet ECs and cultured islets without intraislet ECs, we aimed to determine if DIECs improve the revascularization rate and/or the vascular density of fresh islet grafts compared to cultured islet grafts. The use of fresh or cultured islets for transplantation is a question with high clinical relevance. Although the Edmonton protocol involves transplantation of freshly isolated islets, several arguments have been made for culturing of islets prior to transplantation (135).

4.2.2 DIECs form functional blood vessels after islet transplantation

To investigate if DIECs participate in formation of blood vessels after islet transplantation, freshly isolated Tie2-GFP islets were transplanted under the kidney capsule of nude mice. TPLSM imaging of intact islet grafts using the *ex vivo* model one month after transplantation, a time-point at which the revascularization process is complete (60-62), revealed GFP fluorescent DIECs within the islet grafts. DIECs were located as individual cells and in cell aggregates that formed vessel-like structures (Paper II, Figure 3). Detailed morphological investigations showed that DIECs participated in the formation of large vessels found in the stromal area of the grafts (Paper II, Figure 3; Paper III, Figure 1). Remarkably, segments up to several hundred micrometers of these large vessels were solely composed of DIECs. DIECs also participated in formation of smaller vessels, both in the stromal and endocrine areas of the grafts (Paper II, Figure 3; Paper III, Figure 1). To assess the functionality of DIEC derived vessel structures, graft-bearing kidneys were perfused with Texas Red via the renal artery. Perfusion with Texas Red revealed that DIEC derived vessel structures

were integrated with vessels derived from recipient ECs in the graft vasculature, which was connected to the circulatory system of the kidney (Paper II, Figure 4; Paper III, Figure 1). To investigate if DIECs remained in islet grafts over longer time-periods, freshly isolated Tie2-GFP islets transplanted under the kidney capsule were studied five months after transplantation. *Ex vivo* imaging revealed that DIEC derived vessels were found to have a similar morphology in five months old islet grafts as in one month old islet grafts, indicating that DIECs remain integrated in the vasculature. In addition, perfusion of graft-bearing kidneys with Texas Red showed that DIEC derived vessels were functionally integrated five months after transplantation (Paper III, Figure 1). After the transplantation of Tie2-GFP islets that had been cultured four days, *ex vivo* imaging one month after transplantation showed that only a few DIECs could be found within the cultured islet grafts (not shown).

To further investigate the capability of DIECs to form functional blood vessels, Tie2-GFP islets were transplanted to the anterior chamber of the eye. After transplantation of freshly isolated islets, DIECs participated in the formation of blood vessels that were integrated into the circulatory system as evidenced from perfusion with Texas Red administered into the blood stream. DIEC derived vessel structures were found in the islets and in the intersections between islets and iris (Paper III, Figure 3). Remarkably, DIECs were also found to form long vessel segments of large vessels located in the iris. After transplantation of cultured islets to the anterior chamber, only a few individual DIECs were found (not shown).

One common observation from both the kidney islet grafts and the anterior chamber engrafted islets was that the degree of DIEC contribution was very heterogeneous to different graft regions, i.e. in some graft regions a large number of DIECs were found and in other regions no DIECs were found.

In conclusion, our results show that DIECs have the capacity to participate in the formation of functional blood vessels within the graft vasculature after islet transplantation. Furthermore, the DIECs remained within the islet graft vasculature a long time-period after transplantation, indicating a stable integration. No morphological explanation for the heterogeneous contribution of DIECs to different graft regions was found. Our results confirm the initial observations of Linn et al. (11) that intraislet ECs persist in the islet graft after transplantation of freshly isolated islets. By using another EC specific reporter mouse (lacZ-VEGF receptor 2), Brissova et. al. (67) also showed that DIECs participate in vessel formation after transplantation of freshly isolated islets. Interestingly, the same study also showed that intraislet ECs from human islets transplanted to nude mice contributed to the graft vasculature (67).

4.2.3 DIECs contribute to the vasculature of fresh islet grafts but do not increase total vascularization

The contribution of DIECs to the vasculature was quantified by measuring the vessel area in immunostained kidney islet graft sections. The DIECs contributed to 6% of the vasculature within the endocrine areas of fresh islet grafts, which was significantly higher than in cultured islet grafts where the contribution was only 0.2%. Unexpectedly, DIECs contributed to a greater extent to the vasculature in the stromal graft areas than in endocrine areas, 9% in fresh grafts and 2% in cultured grafts (Paper III, Figure 2). The distribution of DIECs within the grafts was calculated and showed for fresh islet grafts that half of the DIECs were located outside of the endocrine areas,

and for cultured islets grafts that almost all of the DIECs were located outside the endocrine areas (Paper III, Table 1). However, the total area of both donor and recipient vessels in fresh and cultured grafts was similar, both in the endocrine and stromal graft areas. All grafts showed a higher degree of vascularization within the endocrine areas compared to the stromal areas, 12% versus 8% (Paper III, Figure 2).

In conclusion, freshly isolated islets contribute with statistically significant more DIECs to the graft vasculature than cultured islets following islet transplantation. Although, there was a significant contribution of DIECs to fresh islet grafts, the total vascular area of fresh and cultured islet grafts was similar. The finding that freshly isolated islets contribute with more DIECs than cultured islets confirmed the observations from the *ex vivo* imaging. The small contribution of DIECs from cultured islets further suggests that there is a substantial loss of intraislet ECs during islet culture. Unexpectedly, no significant increase in the total vessel area was found in the fresh islet grafts compared to the cultured islet grafts. This could be due to the fact that the number of available ECs provided by the transplanted islets is too limited to have an impact on the total vessel area of the islet grafts. Though, considering that the protein expression of VEGF is upregulated during islet culture (136), cultured islets could have a greater angiogenic capacity that compensates for the lack of intraislet ECs. However, the results may also indicate that the recruitment of ECs during the revascularization of transplanted islets is not a limiting or regulatory factor for the final size of the islet graft vasculature.

Our results contradict the results of Olsson and Carlsson (124), who found that transplantation of freshly isolated islets resulted in islet grafts with a higher vessel density compared to transplantation of cultured islets. However, in the same study it was also reported that the vessel density was two times higher in the stromal graft areas than in the endocrine areas (124). The difference in the vascular morphology of islet grafts in the two studies complicates further interpretations of the diverging results. Interestingly, Brissova et. al. (67) found a much larger contribution of DIECs, 40%, to the islet graft vasculature after transplantation of freshly isolated islets. However, it was not investigated whether the contribution of DIECs effected the vascular density in the islet grafts (67).

4.2.4 Transplantation of freshly isolated islets results in early vessel formation by DIECs and rapid revascularization

To further investigate the contribution of DIECs to the revascularization of transplanted islets, freshly isolated and cultured Tie2-GFP islets were transplanted to the anterior chamber of the eye. Non-invasive TPLSM imaging of the transplanted islets permitted continuous monitoring of the revascularization process (Paper III, Figure 3 and 4). Imaging of islets at the third day after transplantation showed that only few vessels penetrated into peripheral regions of the engrafted islets. However, DIECs participated in vessel formation in the intersections between freshly isolated islets and the iris. Furthermore, round cells with GFP fluorescence were found mainly in the freshly isolated islets. The round cells were found individually and in groups, both close to and distant from circulation (Paper III, Figure 3). The presence of round cells was mainly evident at day three after transplantation, a few round cells could be found at day seven but not at any of the later time-points. Imaging of the engrafted islets seven days after transplantation showed that vessels penetrated into central islet regions in a scattered

manner. DIECs were found to contribute to extensive vessel formation in the revascularization of freshly isolated islets. At fourteen days after transplantation, a vascular network had been formed throughout the engrafted islets. Remodeling of DIEC derived vessels was also observed at this time-point. Only a few individual DIECs could be observed to contribute to the revascularization after transplantation of cultured islets. The vessel density increased rapidly until the fourteenth day after transplantation of both fresh and cultures islets (Paper III, Figure 4). However, there was a trend that freshly isolated islets had a higher vessel density both three and seven days post transplantation. At day fourteen, there was a significantly higher vessel density in the freshly isolated islets. The vessel density was similar in the two groups one month post transplantation.

In conclusion, these results show that DIECs contribute to vessel formation early in the revascularization process, before vessels had started to grow into the engrafted islets. Freshly isolated islets were revascularized at a faster rate than the cultured islets, although the vessel density was similar in the two groups after complete revascularization. This is the first study where the contribution of DIECs to the graft vasculature has been studied during the process of revascularization. Interestingly, the images show that DIECs participate in vessel formation already three days after transplantation, and contribute extensively after seven days. In line with previous *in vitro* studies (11), it seems that a large number of DIECs migrate out of the islets within three days after transplantation, see chapter 4.2.5 for discussion. Unfortunately, the intraislet ECs are very thin and have a too weak fluorescence signal to allow quantification of the contribution of DIEC in intact islet grafts. The trend during the process of revascularization was that freshly isolated islets acquired higher vessel densities more quickly than the cultured islets, which was statistically significant at day fourteen. This could be due to the fact that DIECs provide an extra pool of ECs that are easily recruited to vessel formation. Faster revascularization most likely reduces the duration of hypoxia for the endocrine cells and thereby decreases cell death. Consequently, transplantation of fresh islets may result in the survival of an increased β-cell mass compared to transplantation of cultured islets. Increased β-cell mass could explain the higher capability of freshly isolated islets to reverse diabetes compared to cultured islets (124; 137). One month after transplantation the vessel density was similar in the fresh and cultured islet grafts in the anterior chamber of the eye, which is in agreement with the results from the kidney islet grafts. These results further support the idea that the ability of transplanted islets to recruit ECs is not a limiting factor for determining the final size of the islet graft vasculature, though it appears that the rate of vessel formation during the revascularization process might be limiting and can be enhanced by the supplement of ECs. Furthermore, referring to the previous discussion in chapter 4.2.3, the fact that freshly isolated islets revascularize quicker than cultured islets does not support the idea that cultured islets have a greater angiogenic capacity than fresh islets.

4.2.5 A model of DIECs contribution to graft vasculature

Notably, we found that half of the DIECs were located in the stromal areas of the kidney grafts and that many DIECs were located in the iris, both close to and distant from engrafted islets, after transplantation to the anterior chamber of the eye. These findings clearly show that large numbers of DIECs migrate out of the transplanted

islets. Considering that the transplanted islets produce and secrete VEGF-A (64), this finding is unexpected. However, intraislet ECs have been shown to migrate out of islets *in vitro* when islets are attached to a surface (79; 129; 133; 134) or embedded in a 3D matrix (11; 138). In the 3D matrix, a large number of intraislet ECs have been reported to migrate out of the islets within the first two days (11). Considering both the *in vitro* and the *in vivo* data, it appears as the microenvironment of pancreatic islets no longer provides an adequate milieu for ECs after islet isolation and disruption of vascular connections. This is evident from the fact that the intraislet ECs migrate out of isolated islets to a neighboring surface or tissue if available, or die during islet culture. If freshly isolated islets are transplanted, a large number of intraislet ECs will migrate out of the islets before the recipient vessels starts to penetrate into the islets, i.e. within the first three days after transplantation. During these first days after transplantation, the DIECs are recruited to the processes of angiogenesis that have been induced in the vascular bed of the transplantation-site by VEGF-A, secreted by the islets. Consequently, a large number of DIECs will contribute to the formation of vessels outside of the engrafted islets.

4.3 HOMOGENEOUS VASCULARIZATION OF KIDNEY ISLET GRAFTS

The vessel area in the endocrine areas of the kidney islet grafts was significantly larger compared to the vessel area in the stromal areas. (Paper III, Figure 2). The distribution of vessels within the grafts also showed that the majority of vessels, 60-70%, were found in the endocrine areas of the grafts, although the endocrine areas only represented 50-60% of the grafts (Paper III, Table 1). This finding contradicts some previous reports, which showed that the stromal areas of kidney grafts were vascularized to a significantly higher degree than the endocrine areas (68; 123; 124). To investigate the vascular anatomy of kidney islet grafts in greater detail, freshly isolated Tie2-GFP islets were transplanted to Tie2-GFP recipients. Thereby, islet grafts that expressed GFP throughout the vasculature were obtained. *Ex vivo* imaging one month after transplantation showed that the engrafted islet mass was homogenously vascularized (Paper III, Figure 5). However, a small sub-set of non-vascularized islet structures were found in the grafts. These structures were also found in graft sections and constituted 8% of the islet mass in grafts studied one month after transplantation. However, non-vascularized islet structures were almost absent in islet grafts studied five months after transplantation.

In conclusion, the combined data from *ex vivo* imaging and immunostained graft sections show that transplantation of islets under the kidney capsule results in homogenously vascularized islet grafts, with a higher vessel area among the endocrine cells compared to the stromal cells. The finding that almost ten percent of the transplanted islets do not become vascularized correlates with findings after islet transplantation to the dorsal skinfold (60). Interestingly, the non-vascularized islets were almost absent 5 months after transplantation, suggesting that non-vascularized cells die off. The observation that kidney islet grafts become homogenously vascularized was recently also made in another study (64), supporting our data. The discrepancy in the descriptions of the vascular anatomy in kidney islet grafts might depend on the use of different staining techniques, or differences in islets or transplantation techniques.

4.4 NON-INVASIVE *IN VIVO* IMAGING OF TRANSPLANTED ISLETS

To enable *in vivo* imaging of transplanted islets, the anterior chamber of the eye was explored as a transplantation site. The anterior chamber of the eye has been frequently used as a transplantation site to study a variety of tissues because it is immune privileged (139). Pancreatic tissue transplanted to the anterior chamber of the eye recruits blood vessels (140-142) and retains both the cytoarchitecture (140; 142), and the proportions of the endocrine cells (141). We decided to transplant pancreatic islets into the anterior chamber of the eye because the cornea acts as a natural body window that allows non-invasive *in vivo* imaging of engrafted tissue.

To investigate the engraftment of pancreatic islets in the anterior chamber of the eye, isolated islets were injected into the chamber through the cornea and were found to attach on the iris. Immunostaining of tissue sections with engrafted islets showed that the islets stably engrafted on the iris. Additionally, the proportion of β- and α-cells remained similar in engrafted islets compared to islets located *in situ* in the pancreas (Paper IV, Figure 1). To investigate if islets transplanted to the anterior chamber of the eye recruited blood vessels and to explore the feasibility for *in vivo* imaging, pilot studies were conducted. The transplanted islets were imaged one month after transplantation and FITC-dextran 10 kDa was intravenously administered to visualize the vasculature. The results from these preliminary studies showed that islets engrafted in the anterior chamber of the eye recruited blood vessels and could be imaged *in vivo*.

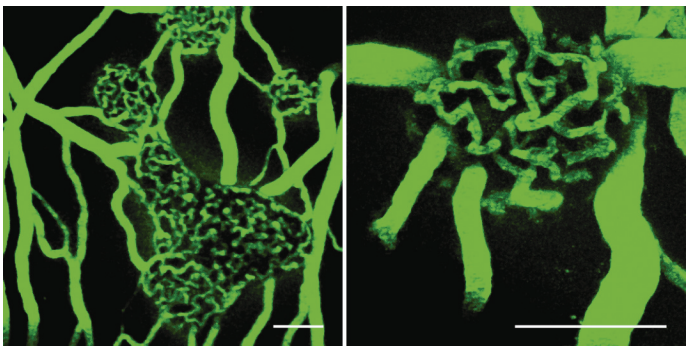

Figure 4. Image projections of islets engrafted in the anterior chamber of the eye. The fluorescence of FITC in the circulation visualizes blood vessels in the iris and in the engrafted islets. The left image show an area of the iris where several individual islets and one islet cluster have engrafted. The right image shows the vasculature of one individually engrafted islet. Scale bars, 100μm

4.4.1 Imaging of β-cells in transplanted islets

By transplanting RIP-GFP islets to the anterior chamber of the eye, we investigated the feasibility of imaging β-cell expression of GFP. Transplanted islets could be readily observed through the cornea in both normal and fluorescence light (Paper IV, Figure 1). TPLSM facilitated high resolution imaging and optical sectioning of the GFP fluorescent β-cells in engrafted RIP-GFP islets, which provided detailed information of islet morphology (Paper IV, Figure 2). Repetitive imaging facilitated longitudinal studies of the engraftment of RIP-GFP islet after transplantation (Paper IV, Figure 3). Transplanted islets engrafted as individual islets or in groups as islet clusters. At day three after transplantation, the islets attached to the iris and showed similar morphology

as prior to transplantation. At day seven, the islets appeared wider and thinner compared to the third day, indicating further attached and spreading onto the iris. Only minor rearrangements of the morphology of the engrafted islets were observed following the seventh day after transplantation. RIP-GFP islet grafts were imaged up to four months after transplantation and retained a similar morphology throughout the time-course.

In conclusion, β-cell expression of GFP was readily imaged at all time-points after transplantation and provided detailed information of the arrangement of β-cells and the morphology of engrafted RIP-GFP islets. The transplanted islets engrafted on the iris and the major morphological rearrangements took place during the first week following transplantation, which is similar to other transplantation-sites (59). The RIP-GFP islet grafts displayed a stable engraftment during the entire length of the study, i.e. four months. The ability to image β-cell gene expression offers the possibility of imaging genetically encoded reporter proteins, as discussed in chapter 1.5.2, for investigations of β-cell signal-transduction, as well as for studies of the other islet cells *in vivo*.

4.4.2 Monitoring of islet revascularization

To investigate the feasibility to monitor the dynamic process of islet revascularization, RIP-GFP islets were transplanted to the anterior chamber of the eye. To visualize the vasculature of the iris and engrafted islets, Texas Red was intravenously injected via the tail vein prior to imaging. TPLSM facilitated simultaneous imaging of GFP fluorescent β-cells and circulating Texas Red. Non-invasive imaging allowed repetitive imaging of the islet graft vasculature day three, seven, fourteen and one month after transplantation (Paper IV, Figure 3). At day three, structural rearrangements of iris vessels close to transplanted islets were observed and ingrowth of a few vessels where found in the peripheral regions of islets. At day seven, more vessels grew into the peripheral regions of the engrafted islets and loops of capillaries started to penetrate into central regions. However, the vessels were scattered in the islets and large islet regions still lacked vessels. At day fourteen, blood vessels formed a microvascular network throughout the engrafted islets. From day fourteen to one month after transplantation, the vessel density increased further in the engrafted islets. One month after transplantation the vasculature was characterized by highly tortuous and uniformly sized capillaries. The vessel density increased continuously during revascularization and the vessel diameter was determined to around eight micrometers (Paper IV, Figure 3). Imaging of the engrafted islets at two and four months after transplantation showed that the vascular morphology was similar to that obtained one month after transplantation.

In conclusion, our results show that non-invasive TPLSM imaging of islets transplanted to the anterior chamber of the eye facilitates longitudinal studies of islet revascularization, simultaneous with imaging of islet morphology. The process of revascularization had started at day three after transplantation, although only with limited ingrowth of vessels to the peripheral regions of the engrafted islets. The major part of vessel ingrowth took part between day three and fourteen after transplantation, with vessels that started to penetrate the islet core at day seven and forming a homogeneous network at day 14. The vessel density increased until one month after transplantation but was then similar at later time-points, indicating that the

revascularization of the islets engrafted in the anterior chamber is completed within one month after transplantation. The vessel diameter was ~8 μm one month after transplantation.

Longitudinal studies of islet revascularization has previously been facilitated by intravital imaging of islets transplanted into the dorsal skinfold chamber (112), and by imaging of islets transplanted under the kidney capsule (62). Studies of islets transplanted to the dorsal skinfold chamber report a similar pattern of islet revascularization as observed in islets transplanted to the anterior chamber of the eye. The revascularization in the dorsal skinfold chamber appears to be complete within 10 days in most cases (61), although increases in the vessel density has been reported until 20 days post transplantation (60). The morphology of the islet graft vasculature and the vessel diameter, between 6 to 9 μm (60; 61), appears very similar in islets engrafted in the dorsal skinfold chamber and in islets engrafted in the anterior chamber of the eye. For islets transplanted under the kidney capsule, the revascularization was also reported to take 20 days (62).

4.4.3 Imaging of β-cell death

To investigate the feasibility of non-invasive imaging of β-cell death, we transplanted RIP-GFP islets into the anterior chamber of the eye, and after completed engraftment and revascularization, we monitored cell death with intravenously administered annexin V-APC. Transplanted RIP-GFP islets imaged in mice with regular blood glucose levels displayed normal morphology and absence of annexin V-APC labeling (Paper IV, Figure 4). Annexin V-APC was found to label a few cells in 1 out of 10 RIP-GFP islet grafts (data not shown). We induced β-cell death in transplanted mice by intravenous administration of alloxan, which rendered mice hyperglycemic one day after injections. At this time-point, substantial loss of GFP fluorescence and structural changes in the reflection of the islet grafts were observed (Paper IV, Figure 4). Administration of annexin V-APC one day after the induction of cell death resulted in labeling of islet grafts. High magnification imaging revealed that most annexin V-APC labeling was found in graft regions devoid of GFP fluorescence, but annexin V-APC fluorescence was also found on the surface of GFP-fluorescent β-cells, indicating labeling of cells undergoing apoptosis (Paper IV, Figure 5). Although a massive β-cell death was obvious in several grafts, the degree of annexin V-APC labeling varied between the grafts indicating a variation in the number of dead or dying cells (Paper IV, Figure 5).

In conclusion, our results show the feasibility of detecting and monitoring β-cell death in islets transplanted to the anterior chamber of the eye. Combined imaging of β-cells, annexin V and reflection provided detailed information regarding the engrafted islets. Imaging of engrafted RIP-GFP islets under normal conditions resulted in annexin V-APC labeling of only a few cells in one graft, indicating a low incidence of cell death in islets transplanted to the anterior chamber of the eye. Systemic administration of alloxan caused β-cell death in islets engrafted into the anterior chamber of the eye, as well as in the pancreas as evidenced by the hyperglycemic blood glucose levels. Loss of GFP fluorescence was evident after alloxan administration, showing that RIP-GFP fluorescence alone could serve as a marker of high levels of β-cell death. Annexin V-APC clearly labeled the engrafted islets after the induction of cell death. The observed variation in annexin V labeling of different grafts, suggests variations in the rates of induction of cell death and/or clearance of dead cells. Annexin V-APC labeling was

found in areas between GFP fluorescent β-cells but also on what appeared as the surface of β-cells. However, since no marker for cell membrane integrity was applied, different stages of apoptosis and necrosis could not be distinguished from each other. The fact that alloxan induced β-cell death in islets transplanted to the anterior chamber of the eye also shows that β-cells in the engrafted islets have a high expression of GLUT2 (143; 144). Noteworthy is that we can now image β-cell death non-invasively and longitudinally under *in vivo* conditions in transplanted islets.

Annexin V binds with high affinity to phosphatidylserine, which translocates from the inner to the outer cell leaflet of the plasma membrane early in apoptosis (145). Annexin V has been validated as an early marker for β-cell apoptosis *in vitro* in dispersed islet cells (146). Furthermore, following chemically induced β-cell death and systemic administration of annexin V in mice, annexin V was confirmed to bind to apoptotic cells by double labeling with markers for apoptosis in pancreatic sections (108). This result strongly supports the use of annexin V as marker for β-cell apoptosis and death *in vivo.*

5 CONCLUDING REMARKS

Novel experimental platforms have been developed that facilitate LSM imaging of islet cells under *in vivo* conditions after pancreatic islet transplantation. These experimental platforms enable functional *in vivo* investigations of β-cell physiology and islet revascularization. The following specific conclusions can be made;

- The YC-3.0 reporter mouse constitutes a novel source of fluorescent- and well-functioning pancreatic islets.

- Intraislet ECs remain in pancreatic islets after islet isolation but rapidly disappear during islet culture. Intraislet ECs participate in blood vessel formation and islet revascularization after pancreatic islet transplantation.

- DIECs significantly contribute to the vasculature of fresh but not cultured islet grafts. However, the total vascular density of fresh and cultured islet grafts is similar after complete revascularization. After transplantation of freshly isolated islets, DIECs participate in early vessel formation and the revascularization is more rapid compared to cultured islets, indicating a shorter period of ischemia for fresh islets after transplantation.

- Pancreatic islets transplanted to the anterior chamber of the eye retain cellular composition, become engrafted and revascularized in a process that can be monitored by non-invasive *in vivo* LSM imaging.

- Transplantation of pancreatic islets with β-cell specific expression of GFP facilitates non-invasive *in vivo* imaging of β-cells and the morphology of islets engrafted in the anterior chamber of the eye. Furthermore, β-cell death can be non-invasively monitored in transplanted islets during normal and diabetic conditions.

By conducting *in vivo* investigations of β-cell signal-transduction in the context of the transplanted islet, then not only surrounded by the other endocrine islet cells but also being vascularized and innervated, we believe that a greater understanding of pancreatic β-cell physiology can be achieved. In addition, this will also contribute unique knowledge concerning β-cell function after transplantation.

6 ACKNOWLEDGEMENTS

An exiting journey has reached its last chapter. During these years I have been fortunate to meet, interact and become inspired by fantastic people both in my scientific and personal life. I would like to express my gratitude to the people who have guided, contributed, helped and cheered me up during these years.

First, I would like to thank my supervisor Per-Olof Berggren for sharing his vast knowledge of science and related matters. He has introduced me to this fascinating field of research and has constantly shared his enthusiasm and visions. I highly appreciate the support and freedom that I have been given to explore my own ideas. Many thanks!

I would like to thank all present and former colleagues at the Rolf Luft Research Center for Diabetes and Endocrinology and at the Department for Molecular Medicine and Surgery for contributing to a unique working environment, and especially:

Martin Köhler, for introducing me to fluorescence microscopy, constant technical support, and for five good years with constant ideas and discussions.

Stephan Speier, for joining the struggle and adventure of in vivo imaging. Also thanks for good chats in the office and in the pub!

Ingo Leibiger, for sharing vast knowledge of cell biology and sharp comments. Tilo Moede, for continuous work and help. Helene Wahlstedt for great project work!

Katarina Breitholtz, Britt-Marie Witasp, Christina Bremer and Lennart Helleday for providing invaluable help and administrative assistance.

Annika Lindgren and Hanne-Lore Rotter for keeping the lab running and fun talks.

The lab girls: Jenny Johansson for after-work beers and discussions, Nancy Wenna-Dekki for laughs and moijitos at South Beach, Rebecka Nilsson and Slavena Mandic for fun lunches and discussions. Jelena Petrovic for actually talking more than me.

Lisa Juntti-Berggren for all that energy, Christoffer Illies for lunch company, Dominic Luc-Webb for the conversations, Essam Refai for fun company in Athens, Sabine Uhles, Jia Yun, Kerstin Brismar, Chris Barker, Barbara Leibiger, Gabriella Imreh, Christina Bark, Pilar Vaca-Sanchez, Vladimir Sharoyko, Sergej Zaitsev, Irina Zaitseva, Luo-Sheng Li, Mikael Turunen, Per Moberg, Stefania Cottá-Doné, Rafael Kramer, Shao-Nian Yang, Juliette Janson, Lena Lilja, Roberta Flume, Elisabeth Noren, Jacob Grünler, Robert Brännström.

All the staff at AKM; Kicki Edwardsson for always finding a solution, Cecilia Brodding, Mirre, Kickan, Sandra, Natalie, Anna-Lena and others, you made it possible!

All the people I have had the pleasure to meet at the DRI in Miami, especially;

Over for being a great host and a generous person, introducing Cuban coffee to me and sharing endless scientific discussions. Alejandro for great laughs and inspiring enthusiasm, as well as for a fruitful collaboration and sharing your scientific knowledge. Camilio Ricordi for giving me the opportunity to visit the DRI, interesting discussions and much appreciated help. Luca Inverardi for sharing your scientific knowledge. Carol for great help and rides.

All co-authors at the Department of Medical Cell Biology, Uppsala University;
Leif Jansson for introducing me to animal surgery, sharing your knowledge and interest about islet revascularization, Britta Bodin and Astrid Nordin for hands on instructions. Also many thanks to Göran Mattson, Arne Andersson and Per-Ola Carlsson.

The UGSBR-friends, you guys are always inspiring and fun! Sarah for a great friendship and your eagerness to promote Canada (and prof-reading), Olle for skiing, training, beers and everlasting scientific discussions, Johanna for being an amazing girl, Erik for all the visions, Lisa the coolest brain surgeon at KS, Katja, Peetra, Benjamin.

The KI guys, Micke for skiing, spinning and beers, Alex for lunches and discussions.

All my great friends in Stockholm for cheerful sailing, kajaking, dinners and drinks!

The Umeå-guys, Pelle, Stefan and Pär, for a great start and always happy reunions.

The old mates from E-town, Pierre, Jocke, Markus Henke and Daniel, for the simplicity of friendship without demands, and for the parties, beers and bullshit.

The family of Rossön: Björkman-Östman, for always cheerful and active gatherings.

In memory of my grandparents who did not get the chance to read this last chapter. For your love and support, I wish I could have shared this moment with you.

I would like to express my deepest gratitude to my sister and my parents, for your unconditional love and support. Your sincere interest and continuous encouragement in all I do never ceases to amaze me.

Finally, Martina, you bring everyday energy and inspiration to my work and life. I'm grateful for your love and support during these years and I'm looking forward to exploring new adventures with you, I love you!

During this thesis work I have received support from the following sources and I would like to express my gratitude; the Lars-Erik Gelin Memorial Foundation, the Swedish Society for Diabetology, the Swedish Society of Medicine, Karolinska Institutet, Swedish Society for Medical Research, Keystone Symposia NIDDKD, Erik and Edith Fernströms Foundation for medical research. This work was additionally supported by the JDRF innovative grant 5-2005-1277, grant DK-58508 from the National Institutes of Health, the Swedish Research Council, the Novo Nordisk Foundation, Karolinska Institutet, the Swedish Diabetes Association, Berth von Kantzow's Foundation, the Family Erling-Persson Foundation and the Diabetes Research Institute Foundation.

7 REFERENCES

1. Mathis D, Vence L, Benoist C: beta-Cell death during progression to diabetes. *Nature* 414:792-798, 2001
2. Prentki M, Nolan CJ: Islet beta cell failure in type 2 diabetes. *J Clin Invest* 116:1802-1812, 2006
3. Kahn SE, Hull RL, Utzschneider KM: Mechanisms linking obesity to insulin resistance and type 2 diabetes. *Nature* 444:840-846, 2006
4. WHO: http://www.who.int/mediacentre/factsheets/fs312/en/.
5. Shapiro AM, Ricordi C, Hering BJ, Auchincloss H, Lindblad R, Robertson RP, Secchi A, Brendel MD, Berney T, Brennan DC, Cagliero E, Alejandro R, Ryan EA, DiMercurio B, Morel P, Polonsky KS, Reems JA, Bretzel RG, Bertuzzi F, Froud T, Kandaswamy R, Sutherland DE, Eisenbarth G, Segal M, Preiksaitis J, Korbutt GS, Barton FB, Viviano L, Seyfert-Margolis V, Bluestone J, Lakey JR: International trial of the Edmonton protocol for islet transplantation. *N Engl J Med* 355:1318-1330, 2006
6. Shapiro AM, Lakey JR, Ryan EA, Korbutt GS, Toth E, Warnock GL, Kneteman NM, Rajotte RV: Islet transplantation in seven patients with type 1 diabetes mellitus using a glucocorticoid-free immunosuppressive regimen. *N Engl J Med* 343:230-238, 2000
7. Ryan EA, Paty BW, Senior PA, Bigam D, Alfadhli E, Kneteman NM, Lakey JR, Shapiro AM: Five-year follow-up after clinical islet transplantation. *Diabetes* 54:2060-2069, 2005
8. Paty BW, Bonner-Weir S, Laughlin MR, McEwan AJ, Shapiro AM: Toward development of imaging modalities for islets after transplantation: insights from the National Institutes of Health Workshop on Beta Cell Imaging. *Transplantation* 77:1133-1137, 2004
9. Jansson L, Carlsson PO: Graft vascular function after transplantation of pancreatic islets. *Diabetologia* 45:749-763, 2002
10. Menger MD, Yamauchi J, Vollmar B: Revascularization and microcirculation of freely grafted islets of Langerhans. *World J Surg* 25:509-515, 2001
11. Linn T, Schneider K, Hammes HP, Preissner KT, Brandhorst H, Morgenstern E, Kiefer F, Bretzel RG: Angiogenic capacity of endothelial cells in islets of Langerhans. *Faseb J* 17:881-883, 2003
12. Köhler M, Nyqvist D, Moede T, Wahlstedt H, Cabrera C, Leibiger IB, Berggren PO: Imaging of Pancreatic Beta-Cell Signal-Transduction. *Curr.Med.Chem.-Immun., Endoc.& Metab. Agents* 4:281-299, 2004
13. Philipson LH, Roe MW: Imaging Metabolic and Signaling Targets in the Pancreatic Beta Cell. *Curr.Med.Chem.-Immun., Endoc.& Metab. Agents* 4:333-337, 2004
14. Jain RK, Munn LL, Fukumura D: Dissecting tumour pathophysiology using intravital microscopy. *Nat Rev Cancer* 2:266-276, 2002
15. Svoboda K, Yasuda R: Principles of two-photon excitation microscopy and its applications to neuroscience. *Neuron* 50:823-839, 2006
16. Dunn KW, Sandoval RM, Molitoris BA: Intravital imaging of the kidney using multiparameter multiphoton microscopy. *Nephron Exp Nephrol* 94:e7-11, 2003
17. Cejvan K, Coy DH, Efendic S: Intra-islet somatostatin regulates glucagon release via type 2 somatostatin receptors in rats. *Diabetes* 52:1176-1181, 2003
18. Rahier J, Goebbels RM, Henquin JC: Cellular composition of the human diabetic pancreas. *Diabetologia* 24:366-371, 1983
19. Ravier MA, Guldenagel M, Charollais A, Gjinovci A, Caille D, Sohl G, Wollheim CB, Willecke K, Henquin JC, Meda P: Loss of connexin36 channels alters beta-cell coupling, islet synchronization of glucose-induced Ca2+ and insulin oscillations, and basal insulin release. *Diabetes* 54:1798-1807, 2005
20. Orci L: Macro- and micro-domains in the endocrine pancreas. *Diabetes* 31:538-565, 1982
21. Orci L, Unger RH: Functional subdivision of islets of Langerhans and possible role of D cells. *Lancet* 2:1243-1244, 1975
22. Brissova M, Fowler MJ, Nicholson WE, Chu A, Hirshberg B, Harlan DM, Powers AC: Assessment of human pancreatic islet architecture and composition by laser scanning confocal microscopy. *J Histochem Cytochem* 53:1087-1097, 2005

23. Cabrera O, Berman DM, Kenyon NS, Ricordi C, Berggren PO, Caicedo A: The unique cytoarchitecture of human pancreatic islets has implications for islet cell function. *Proc Natl Acad Sci U S A* 103:2334-2339, 2006
24. Konstantinova I, Lammert E: Microvascular development: learning from pancreatic islets. *Bioessays* 26:1069-1075, 2004
25. Jansson L: The regulation of pancreatic islet blood flow. *Diabetes Metab Rev* 10:407-416, 1994
26. Jansson L, Hellerstrom C: Stimulation by glucose of the blood flow to the pancreatic islets of the rat. *Diabetologia* 25:45-50, 1983
27. Carlsson PO, Olsson R, Kallskog O, Bodin B, Andersson A, Jansson L: Glucose-induced islet blood flow increase in rats: interaction between nervous and metabolic mediators. *Am J Physiol Endocrinol Metab* 283:E457-464, 2002
28. Nikolova G, Jabs N, Konstantinova I, Domogatskaya A, Tryggvason K, Sorokin L, Fassler R, Gu G, Gerber HP, Ferrara N, Melton DA, Lammert E: The vascular basement membrane: a niche for insulin gene expression and Beta cell proliferation. *Dev Cell* 10:397-405, 2006
29. Kaido T, Yebra M, Cirulli V, Rhodes C, Diaferia G, Montgomery AM: Impact of defined matrix interactions on insulin production by cultured human beta-cells: effect on insulin content, secretion, and gene transcription. *Diabetes* 55:2723-2729, 2006
30. Kamba T, Tam BY, Hashizume H, Haskell A, Sennino B, Mancuso MR, Norberg SM, O'Brien SM, Davis RB, Gowen LC, Anderson KD, Thurston G, Joho S, Springer ML, Kuo CJ, McDonald DM: VEGF-dependent plasticity of fenestrated capillaries in the normal adult microvasculature. *Am J Physiol Heart Circ Physiol* 290:H560-576, 2006
31. Li X, Zhang L, Meshinchi S, Dias-Leme C, Raffin D, Johnson JD, Treutelaar MK, Burant CF: Islet microvasculature in islet hyperplasia and failure in a model of type 2 diabetes. *Diabetes* 55:2965-2973, 2006
32. Ahren B: Autonomic regulation of islet hormone secretion--implications for health and disease. *Diabetologia* 43:393-410, 2000
33. Ahren B, Wierup N, Sundler F: Neuropeptides and the regulation of islet function. *Diabetes* 55 Suppl 2:S98-S107, 2006
34. Matschinsky FM, Glaser B, Magnuson MA: Pancreatic beta-cell glucokinase: closing the gap between theoretical concepts and experimental realities. *Diabetes* 47:307-315, 1998
35. Ashcroft FM, Proks P, Smith PA, Ammala C, Bokvist K, Rorsman P: Stimulus-secretion coupling in pancreatic beta cells. *J Cell Biochem* 55 Suppl:54-65, 1994
36. Berggren PO, Larsson O: Ca2+ and pancreatic B-cell function. *Biochem Soc Trans* 22:12-18, 1994
37. Rutter GA: Nutrient-secretion coupling in the pancreatic islet beta-cell: recent advances. *Mol Aspects Med* 22:247-284, 2001
38. Dyachok O, Isakov Y, Sagetorp J, Tengholm A: Oscillations of cyclic AMP in hormone-stimulated insulin-secreting beta-cells. *Nature* 439:349-352, 2006
39. Itoh Y, Kawamata Y, Harada M, Kobayashi M, Fujii R, Fukusumi S, Ogi K, Hosoya M, Tanaka Y, Uejima H, Tanaka H, Maruyama M, Satoh R, Okubo S, Kizawa H, Komatsu H, Matsumura F, Noguchi Y, Shinohara T, Hinuma S, Fujisawa Y, Fujino M: Free fatty acids regulate insulin secretion from pancreatic beta cells through GPR40. *Nature* 422:173-176, 2003
40. Steneberg P, Rubins N, Bartoov-Shifman R, Walker MD, Edlund H: The FFA receptor GPR40 links hyperinsulinemia, hepatic steatosis, and impaired glucose homeostasis in mouse. *Cell Metab* 1:245-258, 2005
41. Wierup N, Sundler F: CART is a novel islet regulatory peptide. *Peptides* 27:2031-2036, 2006
42. Wendt A, Birnir B, Buschard K, Gromada J, Salehi A, Sewing S, Rorsman P, Braun M: Glucose inhibition of glucagon secretion from rat alpha-cells is mediated by GABA released from neighboring beta-cells. *Diabetes* 53:1038-1045, 2004
43. Ishihara H, Maechler P, Gjinovci A, Herrera PL, Wollheim CB: Islet beta-cell secretion determines glucagon release from neighbouring alpha-cells. *Nat Cell Biol* 5:330-335, 2003

44. Kulkarni RN, Bruning JC, Winnay JN, Postic C, Magnuson MA, Kahn CR: Tissue-specific knockout of the insulin receptor in pancreatic beta cells creates an insulin secretory defect similar to that in type 2 diabetes. *Cell* 96:329-339, 1999
45. Leibiger IB, Leibiger B, Berggren PO: Insulin feedback action on pancreatic beta-cell function. *FEBS Lett* 532:1-6, 2002
46. Valdeolmillos M, Gomis A, Sanchez-Andres JV: In vivo synchronous membrane potential oscillations in mouse pancreatic beta-cells: lack of co-ordination between islets. *J Physiol* 493 (Pt 1):9-18, 1996
47. Sanchez-Andres JV, Gomis A, Valdeolmillos M: The electrical activity of mouse pancreatic beta-cells recorded in vivo shows glucose-dependent oscillations. *J Physiol* 486 (Pt 1):223-228, 1995
48. Fernandez J, Valdeolmillos M: Synchronous glucose-dependent [Ca(2+)](i) oscillations in mouse pancreatic islets of Langerhans recorded in vivo. *FEBS Lett* 477:33-36, 2000
49. Moberg L, Johansson H, Lukinius A, Berne C, Foss A, Kallen R, Ostraat O, Salmela K, Tibell A, Tufveson G, Elgue G, Nilsson Ekdahl K, Korsgren O, Nilsson B: Production of tissue factor by pancreatic islet cells as a trigger of detrimental thrombotic reactions in clinical islet transplantation. *Lancet* 360:2039-2045, 2002
50. Johansson H, Lukinius A, Moberg L, Lundgren T, Berne C, Foss A, Felldin M, Kallen R, Salmela K, Tibell A, Tufveson G, Ekdahl KN, Elgue G, Korsgren O, Nilsson B: Tissue factor produced by the endocrine cells of the islets of Langerhans is associated with a negative outcome of clinical islet transplantation. *Diabetes* 54:1755-1762, 2005
51. Ballinger WF, Lacy PE: Transplantation of intact pancreatic islets in rats. *Surgery* 72:175-186, 1972
52. Evgenov NV, Medarova Z, Dai G, Bonner-Weir S, Moore A: In vivo imaging of islet transplantation. *Nat Med* 12:144-148, 2006
53. Kim SJ, Doudet DJ, Studenov AR, Nian C, Ruth TJ, Gambhir SS, McIntosh CH: Quantitative micro positron emission tomography (PET) imaging for the in vivo determination of pancreatic islet graft survival. *Nat Med* 12:1423-1428, 2006
54. Fowler M, Virostko J, Chen Z, Poffenberger G, Radhika A, Brissova M, Shiota M, Nicholson WE, Shi Y, Hirshberg B, Harlan DM, Jansen ED, Powers AC: Assessment of pancreatic islet mass after islet transplantation using in vivo bioluminescence imaging. *Transplantation* 79:768-776, 2005
55. Chen X, Zhang X, Larson CS, Baker MS, Kaufman DB: In vivo bioluminescence imaging of transplanted islets and early detection of graft rejection. *Transplantation* 81:1421-1427, 2006
56. Virostko J, Jansen ED, Powers AC: Current status of imaging pancreatic islets. *Curr Diab Rep* 6:328-332, 2006
57. Moritz W, Meier F, Stroka DM, Giuliani M, Kugelmeier P, Nett PC, Lehmann R, Candinas D, Gassmann M, Weber M: Apoptosis in hypoxic human pancreatic islets correlates with HIF-1alpha expression. *Faseb J* 16:745-747, 2002
58. Miao G, Ostrowski RP, Mace J, Hough J, Hopper A, Peverini R, Chinnock R, Zhang J, Hathout E: Dynamic production of hypoxia-inducible factor-1alpha in early transplanted islets. *Am J Transplant* 6:2636-2643, 2006
59. Davalli AM, Scaglia L, Zangen DH, Hollister J, Bonner-Weir S, Weir GC: Vulnerability of islets in the immediate posttransplantation period. Dynamic changes in structure and function. *Diabetes* 45:1161-1167, 1996
60. Beger C, Cirulli V, Vajkoczy P, Halban PA, Menger MD: Vascularization of purified pancreatic islet-like cell aggregates (pseudoislets) after syngeneic transplantation. *Diabetes* 47:559-565, 1998
61. Menger MD, Vajkoczy P, Leiderer R, Jager S, Messmer K: Influence of experimental hyperglycemia on microvascular blood perfusion of pancreatic islet isografts. *J Clin Invest* 90:1361-1369, 1992
62. Merchant FA, Diller KR, Aggarwal SJ, Bovik AC: Angiogenesis in cultured and cryopreserved pancreatic islet grafts. *Transplantation* 63:1652-1660, 1997
63. Vajkoczy P, Olofsson AM, Lehr HA, Leiderer R, Hammersen F, Arfors KE, Menger MD: Histogenesis and ultrastructure of pancreatic islet graft microvasculature. Evidence for graft revascularization by endothelial cells of host origin. *Am J Pathol* 146:1397-1405, 1995

64. Brissova M, Shostak A, Shiota M, Wiebe PO, Poffenberger G, Kantz J, Chen Z, Carr C, Jerome WG, Chen J, Baldwin HS, Nicholson W, Bader DM, Jetton T, Gannon M, Powers AC: Pancreatic islet production of vascular endothelial growth factor--a is essential for islet vascularization, revascularization, and function. *Diabetes* 55:2974-2985, 2006
65. Contreras JL, Smyth CA, Eckstein C, Bilbao G, Thompson JA, Young CJ, Eckhoff DE: Peripheral mobilization of recipient bone marrow-derived endothelial progenitor cells enhances pancreatic islet revascularization and engraftment after intraportal transplantation. *Surgery* 134:390-398, 2003
66. Nyqvist D, Köhler M, Wahlstedt H, Berggren PO: Donor islet endothelial cells participate in formation of functional vessels within pancreatic islet grafts. *Diabetes* 54:2287-2293, 2005
67. Brissova M, Fowler M, Wiebe P, Shostak A, Shiota M, Radhika A, Lin PC, Gannon M, Powers AC: Intraislet endothelial cells contribute to revascularization of transplanted pancreatic islets. *Diabetes* 53:1318-1325, 2004
68. Mattsson G, Jansson L, Carlsson PO: Decreased vascular density in mouse pancreatic islets after transplantation. *Diabetes* 51:1362-1366, 2002
69. Carlsson PO, Jansson L, Andersson A, Källskog Ö: Capillary blood pressure in syngeneic rat islets transplanted under the renal capsule is similar to that of the implantation organ. *Diabetes* 47:1586-1593, 1998
70. Carlsson PO, Liss P, Andersson A, Jansson L: Measurements of oxygen tension in native and transplanted rat pancreatic islets. *Diabetes* 47:1027-1032, 1998
71. Carlsson PO, Palm F, Andersson A, Liss P: Markedly decreased oxygen tension in transplanted rat pancreatic islets irrespective of the implantation site. *Diabetes* 50:489-495, 2001
72. Stagner JI, Samols E: The induction of capillary bed development by endothelial cell growth factor before islet transplantation may prevent islet ischemia. *Transplant Proc* 22:824-828, 1990
73. Kawakami Y, Iwata H, Gu Y, Miyamoto M, Murakami Y, Yamasaki T, Cui W, Ikada Y, Imamura M, Inoue K: Modified subcutaneous tissue with neovascularization is useful as the site for pancreatic islet transplantation. *Cell Transplant* 9:729-732, 2000
74. Zhang N, Richter A, Suriawinata J, Harbaran S, Altomonte J, Cong L, Zhang H, Song K, Meseck M, Bromberg J, Dong H: Elevated vascular endothelial growth factor production in islets improves islet graft vascularization. *Diabetes* 53:963-970, 2004
75. Lai Y, Schneider D, Kidszun A, Hauck-Schmalenberger I, Breier G, Brandhorst D, Brandhorst H, Iken M, Brendel MD, Bretzel RG, Linn T: Vascular endothelial growth factor increases functional beta-cell mass by improvement of angiogenesis of isolated human and murine pancreatic islets. *Transplantation* 79:1530-1536, 2005
76. Narang AS, Cheng K, Henry J, Zhang C, Sabek O, Fraga D, Kotb M, Gaber AO, Mahato RI: Vascular endothelial growth factor gene delivery for revascularization in transplanted human islets. *Pharm Res* 21:15-25, 2004
77. Zhang N, Qu S, Xu J, Bromberg JS, Dong HH: Inhibition of angiogenesis is associated with reduced islet engraftment in diabetic recipient mice. *Transplant Proc* 37:4452-4457, 2005
78. Zhang N, Su D, Qu S, Tse T, Bottino R, Balamurugan AN, Xu J, Bromberg JS, Dong HH: Sirolimus is associated with reduced islet engraftment and impaired beta-cell function. *Diabetes* 55:2429-2436, 2006
79. Cantaluppi V, Biancone L, Romanazzi GM, Figliolini F, Beltramo S, Ninniri MS, Galimi F, Romagnoli R, Franchello A, Salizzoni M, Perin PC, Ricordi C, Segoloni GP, Camussi G: Antiangiogenic and immunomodulatory effects of rapamycin on islet endothelium: relevance for islet transplantation. *Am J Transplant* 6:2601-2611, 2006
80. Denk W, Strickler JH, Webb WW: Two-photon laser scanning fluorescence microscopy. *Science* 248:73-76, 1990
81. Conchello JA, Lichtman JW: Optical sectioning microscopy. *Nat Methods* 2:920-931, 2005
82. Gerlich D, Ellenberg J: 4D imaging to assay complex dynamics in live specimens. *Nat Cell Biol* Suppl:S14-19, 2003
83. Helmchen F, Denk W: Deep tissue two-photon microscopy. *Nat Methods* 2:932-940, 2005

84. Zipfel WR, Williams RM, Webb WW: Nonlinear magic: multiphoton microscopy in the biosciences. *Nat Biotechnol* 21:1369-1377, 2003
85. Theer P, Hasan MT, Denk W: Two-photon imaging to a depth of 1000 microm in living brains by use of a Ti:Al2O3 regenerative amplifier. *Opt Lett* 28:1022-1024, 2003
86. Chalfie M, Tu Y, Euskirchen G, Ward WW, Prasher DC: Green fluorescent protein as a marker for gene expression. *Science* 263:802-805, 1994
87. Okabe M, Ikawa M, Kominami K, Nakanishi T, Nishimune Y: 'Green mice' as a source of ubiquitous green cells. *FEBS Lett* 407:313-319, 1997
88. Hadjantonakis AK, Dickinson ME, Fraser SE, Papaioannou VE: Technicolour transgenics: imaging tools for functional genomics in the mouse. *Nat Rev Genet* 4:613-625, 2003
89. Lippincott-Schwartz J, Patterson GH: Development and use of fluorescent protein markers in living cells. *Science* 300:87-91, 2003
90. Shaner NC, Steinbach PA, Tsien RY: A guide to choosing fluorescent proteins. *Nat Methods* 2:905-909, 2005
91. Leibiger B, Moede T, Schwarz T, Brown GR, Köhler M, Leibiger IB, Berggren PO: Short-term regulation of insulin gene transcription by glucose. *Proc Natl Acad Sci U S A* 95:9307-9312, 1998
92. Hara M, Wang X, Kawamura T, Bindokas VP, Dizon RF, Alcoser SY, Magnuson MA, Bell GI: Transgenic mice with green fluorescent protein-labeled pancreatic beta -cells. *Am J Physiol Endocrinol Metab* 284:E177-183, 2003
93. Curran MA, Ochoa MS, Molano RD, Pileggi A, Inverardi L, Kenyon NS, Nolan GP, Ricordi C, Fenjves ES: Efficient transduction of pancreatic islets by feline immunodeficiency virus vectors1. *Transplantation* 74:299-306, 2002
94. Flotte T, Agarwal A, Wang J, Song S, Fenjves ES, Inverardi L, Chesnut K, Afione S, Loiler S, Wasserfall C, Kapturczak M, Ellis T, Nick H, Atkinson M: Efficient ex vivo transduction of pancreatic islet cells with recombinant adeno-associated virus vectors. *Diabetes* 50:515-520, 2001
95. Moede T, Leibiger B, Berggren PO, Leibiger IB: Online monitoring of stimulus-induced gene expression in pancreatic beta-cells. *Diabetes* 50 Suppl 1:S15-19, 2001
96. Hara M, Bindokas V, Lopez JP, Kaihara K, Landa LR, Jr., Harbeck M, Roe MW: Imaging endoplasmic reticulum calcium with a fluorescent biosensor in transgenic mice. *Am J Physiol Cell Physiol* 287:C932-938, 2004
97. Bennett BD, Jetton TL, Ying G, Magnuson MA, Piston DW: Quantitative subcellular imaging of glucose metabolism within intact pancreatic islets. *J Biol Chem* 271:3647-3651, 1996
98. Kotlikoff MI: Genetically encoded Ca2+ indicators: using genetics and molecular design to understand complex physiology. *J Physiol* 578:55-67, 2007
99. Varadi A, Rutter GA: Dynamic imaging of endoplasmic reticulum Ca2+ concentration in insulin-secreting MIN6 Cells using recombinant targeted cameleons: roles of sarco(endo)plasmic reticulum Ca2+-ATPase (SERCA)-2 and ryanodine receptors. *Diabetes* 51 Suppl 1:S190-201, 2002
100. Takahashi N, Nemoto T, Kimura R, Tachikawa A, Miwa A, Okado H, Miyashita Y, Iino M, Kadowaki T, Kasai H: Two-photon excitation imaging of pancreatic islets with various fluorescent probes. *Diabetes* 51 Suppl 1:S25-28, 2002
101. Heim N, Garaschuk O, Friedrich MW, Mank M, Milos RI, Kovalchuk Y, Konnerth A, Griesbeck O: Improved calcium imaging in transgenic mice expressing a troponin C-based biosensor. *Nat Methods* 4:127-129, 2007
102. Palmer AE, Giacomello M, Kortemme T, Hires SA, Lev-Ram V, Baker D, Tsien RY: Ca2+ indicators based on computationally redesigned calmodulin-peptide pairs. *Chem Biol* 13:521-530, 2006
103. Svoboda K, Denk W, Kleinfeld D, Tank DW: In vivo dendritic calcium dynamics in neocortical pyramidal neurons. *Nature* 385:161-165, 1997
104. Stosiek C, Garaschuk O, Holthoff K, Konnerth A: In vivo two-photon calcium imaging of neuronal networks. *Proc Natl Acad Sci U S A* 100:7319-7324, 2003
105. Ohara-Imaizumi M, Nakamichi Y, Tanaka T, Katsuta H, Ishida H, Nagamatsu S: Monitoring of exocytosis and endocytosis of insulin secretory granules in the pancreatic beta-cell line MIN6 using pH-sensitive green fluorescent protein (pHluorin) and confocal laser microscopy. *Biochem J* 363:73-80, 2002

106. Bozza T, McGann JP, Mombaerts P, Wachowiak M: In vivo imaging of neuronal activity by targeted expression of a genetically encoded probe in the mouse. *Neuron* 42:9-21, 2004
107. Köhler M, Zaitsev SV, Zaitseva, II, Leibiger B, Leibiger IB, Turunen M, Kapelioukh IL, Bakkman L, Appelskog IB, de Monvel JB, Imreh G, Berggren PO: On-line monitoring of apoptosis in insulin-secreting cells. *Diabetes* 52:2943-2950, 2003
108. Medarova Z, Bonner-Weir S, Lipes M, Moore A: Imaging beta-cell death with a near-infrared probe. *Diabetes* 54:1780-1788, 2005
109. Dumont EA, Reutelingsperger CP, Smits JF, Daemen MJ, Doevendans PA, Wellens HJ, Hofstra L: Real-time imaging of apoptotic cell-membrane changes at the single-cell level in the beating murine heart. *Nat Med* 7:1352-1355, 2001
110. Bertera S, Geng X, Tawadrous Z, Bottino R, Balamurugan AN, Rudert WA, Drain P, Watkins SC, Trucco M: Body window-enabled in vivo multicolor imaging of transplanted mouse islets expressing an insulin-Timer fusion protein. *Biotechniques* 35:718-722, 2003
111. Vajkoczy P, Menger MD, Simpson E, Messmer K: Angiogenesis and vascularization of murine pancreatic islet isografts. *Transplantation* 60:123-127, 1995
112. Menger MD, Jager S, Walter P, Hammersen F, Messmer K: A novel technique for studies on the microvasculature of transplanted islets of Langerhans in vivo. *Int J Microcirc Clin Exp* 9:103-117, 1990
113. Merchant FA, Aggarwal SJ, Diller KR, Bovik AC: In-vivo analysis of angiogenesis and revascularization of transplanted pancreatic islets using confocal microscopy. *J Microsc* 176 (Pt 3):262-275, 1994
114. Tsai PS, Friedman B, Ifarraguerri AI, Thompson BD, Lev-Ram V, Schaffer CB, Xiong Q, Tsien RY, Squier JA, Kleinfeld D: All-optical histology using ultrashort laser pulses. *Neuron* 39:27-41, 2003
115. Hinegardner RT: An improved fluorometric assay for DNA. *Anal Biochem* 39:197-201, 1971
116. Andersson A, Sandler S: Viability tests of cryopreserved endocrine pancreatic cells. *Cryobiology* 20:161-168, 1983
117. Jansson L: Flow distribution between the endocrine and exocrine parts of the isolated rat pancreas during perfusion in vitro with different glucose concentrations. *Acta Physiol Scand* 126:533-538, 1986
118. Carlsson PO, Jansson L, Östenson CG, Källskog O: Islet capillary blood pressure increase mediated by hyperglycemia in NIDDM GK rats. *Diabetes* 46:947-952, 1997
119. Jansson L, Hellerström C: A rapid method of visualizing the pancreatic islets for studies of islet capillary blood flow using non-radioactive microspheres. *Acta Physiol Scand* 113:371-374, 1981
120. Szkudelski T: The mechanism of alloxan and streptozotocin action in B cells of the rat pancreas. *Physiol Res* 50:537-546, 2001
121. Korsgren O, Jansson L, Andersson A: Effects of hyperglycemia on function of isolated mouse pancreatic islets transplanted under kidney capsule. *Diabetes* 38:510-515, 1989
122. Vecchi A, Garlanda C, Lampugnani MG, Resnati M, Matteucci C, Stoppacciaro A, Schnurch H, Risau W, Ruco L, Mantovani A, et al.: Monoclonal antibodies specific for endothelial cells of mouse blood vessels. Their application in the identification of adult and embryonic endothelium. *Eur J Cell Biol* 63:247-254, 1994
123. Mattsson G, Jansson L, Nordin A, Carlsson PO: Impaired revascularization of transplanted mouse pancreatic islets is chronic and glucose-independent. *Transplantation* 75:736-739, 2003
124. Olsson R, Carlsson PO: Better vascular engraftment and function in pancreatic islets transplanted without prior culture. *Diabetologia* 48:469-476, 2005
125. Miyawaki A, Llopis J, Heim R, McCaffery JM, Adams JA, Ikura M, Tsien RY: Fluorescent indicators for Ca2+ based on green fluorescent proteins and calmodulin. *Nature* 388:882-887, 1997
126. von Seth E, Nyqvist D, Andersson A, Carlsson PO, Köhler M, Mattsson G, Nordin A, Berggren PO, Jansson L: Distribution of Intraportally Implanted Microspheres and Fluorescent islets in mice. *Cell Transplantation In press*, 2007

127. Lau J, Mattsson M, Nyqvist D, Köhler M, Berggren PO, Jansson L, Carlsson PO: Induced dysfunction in intraportally transplanted pancreatic islets by the liver microenvironment. *Submitted manuscript*, 2007
128. Anghelina M, Moldovan L, Moldovan NI: Preferential activity of Tie2 promoter in arteriolar endothelium. *J Cell Mol Med* 9:113-121, 2005
129. Suschek C, Fehsel K, Kroncke KD, Sommer A, Kolb-Bachofen V: Primary cultures of rat islet capillary endothelial cells. Constitutive and cytokine-inducible macrophagelike nitric oxide synthases are expressed and activities regulated by glucose concentration. *Am J Pathol* 145:685-695, 1994
130. Parr EL, Bowen KM, Lafferty KJ: Cellular changes in cultured mouse thyroid glands and islets of Langerhans. *Transplantation* 30:135-141, 1980
131. Olsson R, Maxhuni A, Carlsson PO: Revascularization of transplanted pancreatic islets following culture with stimulators of angiogenesis. *Transplantation* 82:340-347, 2006
132. Mendola JF, Goity C, Fernandez-Alvarez J, Saenz A, Benarroch G, Fernandez-Cruz L, Gomis R: Immunocytochemical study of pancreatic islet revascularization in islet isograft. Effect of hyperglycemia of the recipient and of in vitro culture of islets. *Transplantation* 57:725-730, 1994
133. Biancone L, Cantaluppi V, Romanazzi GM, Russo S, Figliolini F, Beltramo S, Scalabrino E, Deregibus MC, Romagnoli R, Franchello A, Salizzoni M, Perin PC, Ricordi C, Segoloni GP, Camussi G: Platelet-activating factor synthesis and response on pancreatic islet endothelial cells: relevance for islet transplantation. *Transplantation* 81:511-518, 2006
134. Lou J, Triponez F, Oberholzer J, Wang H, Yu D, Buhler L, Cretin N, Mentha G, Wollheim CB, Morel P: Expression of alpha-1 proteinase inhibitor in human islet microvascular endothelial cells. *Diabetes* 48:1773-1778, 1999
135. Ricordi C: Islet transplantation: a brave new world. *Diabetes* 52:1595-1603, 2003
136. Vasir B, Aiello LP, Yoon KH, Quickel RR, Bonner-Weir S, Weir GC: Hypoxia induces vascular endothelial growth factor gene and protein expression in cultured rat islet cells. *Diabetes* 47:1894-1903, 1998
137. King A, Lock J, Xu G, Bonner-Weir S, Weir GC: Islet transplantation outcomes in mice are better with fresh islets and exendin-4 treatment. *Diabetologia* 48:2074-2079, 2005
138. Kidszun A, Schneider D, Erb D, Hertl G, Schmidt V, Eckhard M, Preissner KT, Breier G, Bretzel RG, Linn T: Isolated pancreatic islets in three-dimensional matrices are responsive to stimulators and inhibitors of angiogenesis. *Cell Transplant* 15:489-497, 2006
139. Niederkorn JY: Immune privilege in the anterior chamber of the eye. *Crit Rev Immunol* 22:13-46, 2002
140. Adeghate E, Donath T: Morphological findings in long-term pancreatic tissue transplants in the anterior eye chamber of rats. *Pancreas* 5:298-305, 1990
141. Adeghate E, Ponery AS, Ahmed I, Donath T: Comparative morphology and biochemistry of pancreatic tissue fragments transplanted into the anterior eye chamber and subcutaneous regions of the rat. *Eur J Morphol* 39:257-268, 2001
142. Hultquist GT: The ultrastructure of pancreatic tissue from duct-ligated rats implanted into anterior chamber of rat eyes. *Ups J Med Sci* 77:8-18, 1972
143. De Vos A, Heimberg H, Quartier E, Huypens P, Bouwens L, Pipeleers D, Schuit F: Human and rat beta cells differ in glucose transporter but not in glucokinase gene expression. *J Clin Invest* 96:2489-2495, 1995
144. Elsner M, Tiedge M, Guldbakke B, Munday R, Lenzen S: Importance of the GLUT2 glucose transporter for pancreatic beta cell toxicity of alloxan. *Diabetologia* 45:1542-1549, 2002
145. Fadok VA, Voelker DR, Campbell PA, Cohen JJ, Bratton DL, Henson PM: Exposure of phosphatidylserine on the surface of apoptotic lymphocytes triggers specific recognition and removal by macrophages. *J Immunol* 148:2207-2216, 1992
146. Cattan P, Berney T, Schena S, Molano RD, Pileggi A, Vizzardelli C, Ricordi C, Inverardi L: Early assessment of apoptosis in isolated islets of Langerhans. *Transplantation* 71:857-862, 2001